We are IntechOpen,
the world's leading publisher of
Open Access books
Built by scientists, for scientists

6,900
Open access books available

186,000
International authors and editors

200M
Downloads

Our authors are among the

154
Countries delivered to

TOP 1%
most cited scientists

12.2%
Contributors from top 500 universities

CLARIVATE ANALYTICS
BOOK CITATION INDEX
INDEXED

WEB OF SCIENCE™

Selection of our books indexed in the Book Citation Index
in Web of Science™ Core Collection (BKCI)

Interested in publishing with us?
Contact book.department@intechopen.com

Numbers displayed above are based on latest data collected.
For more information visit www.intechopen.com

Cyclic Voltammetry of Phthalocyanines

Keiichi Sakamoto

Abstract

Phthalocyanines and their related compounds possess similar structures as porphyrins. They have been used as green to blue dyes and pigments since their discovery. In this decade, they are known to be utilized in important functional colorants for many fields such as catalyst, laser light absorbers in data storage systems, electrocharge carriers in photocopies, photo-antenna device in photosynthesis, photovoltaic cells and photosensitizers for dye-sensitized solar cells (DSSCs), and photodynamic therapy of cancer (PDT). The functions are attributed to high electron transfer abilities of phthalocyanines. Cyclic voltammograms were carried out for phthalocyanines in order to estimate their electron transfer abilities and electrochemical mechanism.

Keywords: phthalocyanines, cyclic voltammetry, electrochemistry electron transfer abilities, photosensitizers

1. Introduction

A blue-colored insoluble compound was accidently observed as a by-product at the South Metropolitan Gas Company in London during the preparation of *o*-cyanobenzamide from phthalimide and acetic acid at a high temperature by Braun and Tcherniac in 1907. The compound was later called phthalocyanine. In 1927, at the University of Fribourg, de Diesbach and von der Weid obtained stable blue material during the preparation of phthalonitrile from *o*-dibromobenzene with copper cyanide in refluxing pyridine. Later, the blue material was identified as copper phthalocyanine. In the following year, the blue impurity in the reaction products was formed during the industrial preparation of phthalimide from phthalic anhydride and ammonia in a glass-lined reaction vessel at the Grangemouth plant of Scottish Dyes Ltd. During the preparation, the glass-lined reaction vessel was cracked. By reason of the reaction carried out, outer steel casing of the reaction vessel, the accident results in the formation of blue impurity. This blue impurity is known to iron phthalocyanine at the present [1–5].

These blue materials determined the molecular structure, which was composed of four iminoisoindoline units with various central metal ions or di-hydrogen by Professor R. P. Linstead at University of London in 1929. Linstead named the by-product *phthalocyanine* as a combination of Greek *naphtha* (rock oil) and *cyanine* (blue) in 1933. The molecular structure of phthalocyanine was confirmed later using X-ray diffraction analysis by Robertson in 1935 [1–5].

Phthalocyanine and metal containing phthalocyanines have been established as blue to green dyestuffs and pigments. Phthalocyanines and metal phthalocyanines are using an important industrial commodity since 1942 [1–5].

Phthalocyanines are an analogous molecular structure as natural colorant of porphyrins. In general, porphyrins consist of four pyrrole units, while phthalocyanines construct four isoindole and nitrogen atoms at *meso* positions. The central cavity of phthalocyanines can place 63 different elemental ions including di-hydrogen (metal-free phthalocyanine). Phthalocyanines containing one or two metal ions are called metal phthalocyanines. In phthalocyanine ring system and part of the atom numbering system, the 2,3,9,10,16,17,23,24 positions are referred to as the peripheral sites and the 1,4,8,11,15,18,22,25 positions as the nonperipheral sites. M can be di-hydrogen or one of the 63 elements of the periodic table (**Figure 1**) [1–5].

As mentioned above, phthalocyanines have been used as green to blue colorants in textile industries because of their thermal, chemical, and photochemical stabilities from their discovery. Over the last decade, phthalocyanines have attractive attention as functional chromophores for various fields such as catalyst, laser light absorbers in data storage systems, electron charge carriers in photocopiers,
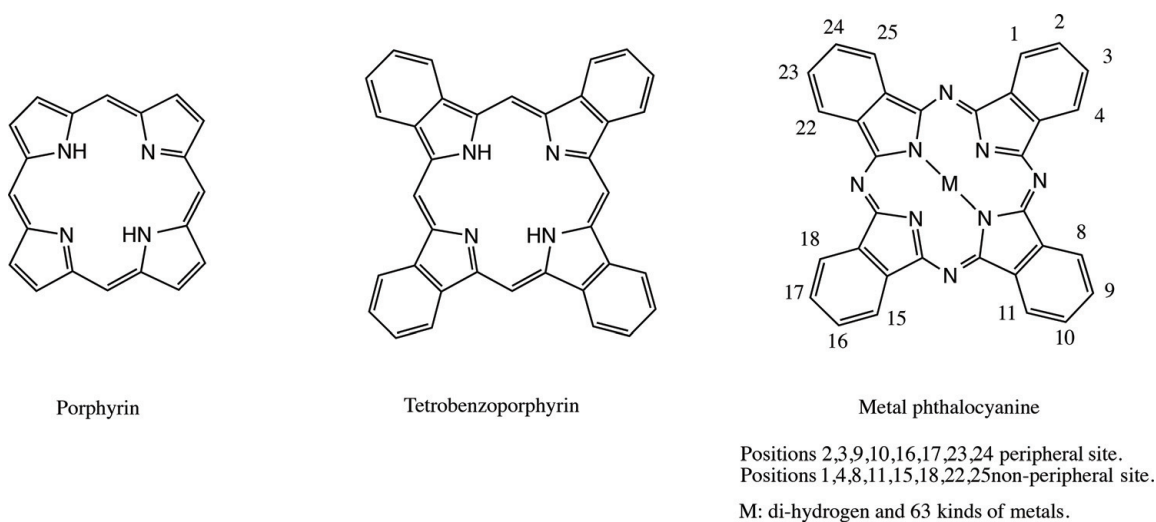
Porphyrin   Tetrobenzoporphyrin   Metal phthalocyanine

Positions 2,3,9,10,16,17,23,24 peripheral site.
Positions 1,4,8,11,15,18,22,25 non-peripheral site.

M: di-hydrogen and 63 kinds of metals.

Figure 1.
Molecular structures of porphyrin, porphyrin-related compound, and metal phthalocyanine.
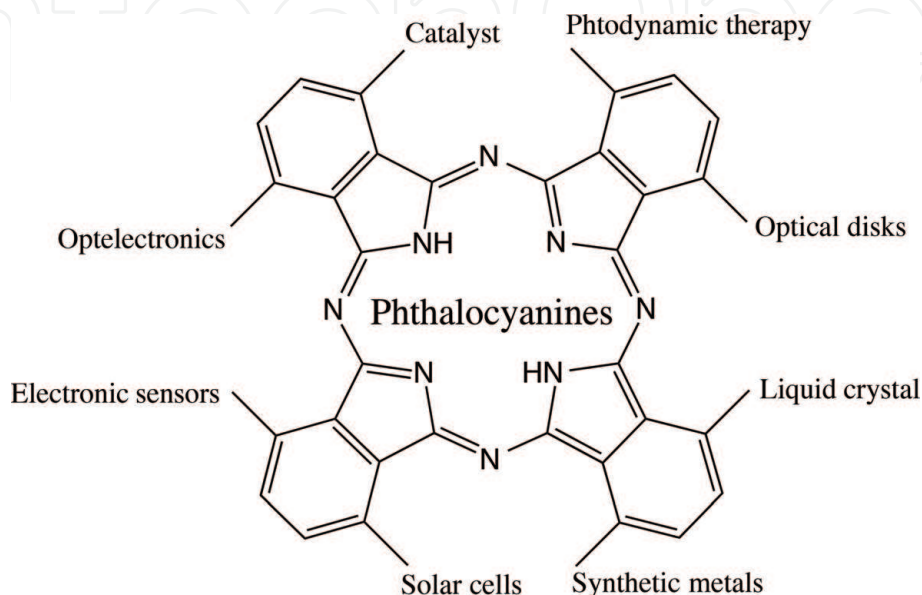
Figure 2.
Typical function of phthalocyanines.

photo-antenna device in photosynthesis, photoconductors in photovoltaic cells, and electrochromic displays, and photosensitizers [6–20] (**Figure 2**).

In order to utilize many applications, the absorption maxima of phthalocyanines are best if moved near infrared region. The strongest absorption of phthalocyanines in visible region called Q band can be attributed to allow from highest occupied molecular orbital (HOMO) to lowest unoccupied molecular orbital (LUMO), which means π–π* transition. The Q-band of phthalocyanines can be moved by bathochromic effect through extension of the π conjugation system. Especially, phthalocyanines having bathochromic effect are useful for photosensitization purposes.

Photosensitization properties of phthalocyanines are utilized for both photo-dynamic therapy of cancer (PDT) and dye-sensitized solar cells (DSSCs) [21].

Particularly, phthalocyanines are known to have the potentials to utilize as second-generation photosensitizers for PDT because they have long life time triplet state and show strong absorption of the far-red light between 600 and 850 nm of which a greater penetration of tissue and satisfactory photosensitization of singlet oxygen take place [21–23].

No-substituted phthalocyanines are insoluble or lower solubility in common organic solvents. The weak points of phthalocyanines have been improved to introduce substituents onto the ring system. Alkyl-substituted phthalocyanines become soluble in organic solvents and they have a lipophilic property. The lipophilic phthalocyanines have a high tumor affinity [24]. Hydrophilic-substituted phthalocyanines show solubility in aqueous media. Phthalocyanines containing pyridine rings in place of one or more of the benzenoid rings expected amphiphilic properties [17].

In the second place, phthalocyanines have attractive attention for the conversion of solar to electricity, because dyes come into general used for DSSCs absorb only weakly in solar spectrum. Phthalocyanines for DSSCs are required to possess strong absorption of visible light in the far-red or near infrared region. Then, phthalocyanines have high conversion capability of solar energy to electricity in comparison to common sensitized dyes [25].

In this chapter, synthesis and cyclic voltammetry of soluble phthalocyanines and their homologs compounds, subphthalocyanines were described in order to utilize photosensitizers for PDT and DSSCs [10, 21].

2. Phthalocyanines

2.1 Synthesized peripheral-substituted phthalocyanines

Synthesized phthalocyanines were the followings: phthalocyanine-4,4′,4″4‴-tetrasulfonic acids having sulfonic groups, phthalocyanine-2,3,9,10,16,17,23,24-octacarboxylic acids having carboxylic groups, 2,3,9,10,16,17,23,24-octakis (hexoxymethyl)phthalocyanines and anthraquinocyanines, which has four 9,10-anthraquinone units in the phthalocyanine molecule [26, 27].

Phthalocyanine-4,4′,4″,4‴-tetrasulfonic acids were synthesized from 4-sulfophthalic acid, a metal halide, urea and 1,8-diazabicyclo[5.4.0]undec-7-ene (DBU) as a catalyst [26] (**Figure 3**).

Phthalocyanine-2,3,9,10,16,17,23,24-octacarboxylic acids were synthesized from benzene-1,2,4,5-tetracarboxylic dianhydride (pyromellitic dianhydride), a metal halide and urea under the reaction conditions used for the monomer preparation [26] (**Figure 4**).

The 2,3,9,10,16,17,23,24-octakis(hexoxymethyl)phthalocyanines were synthesized from 1,2-dicyano-4,5-bis(hexoxymethyl)benzene, which was prepared from
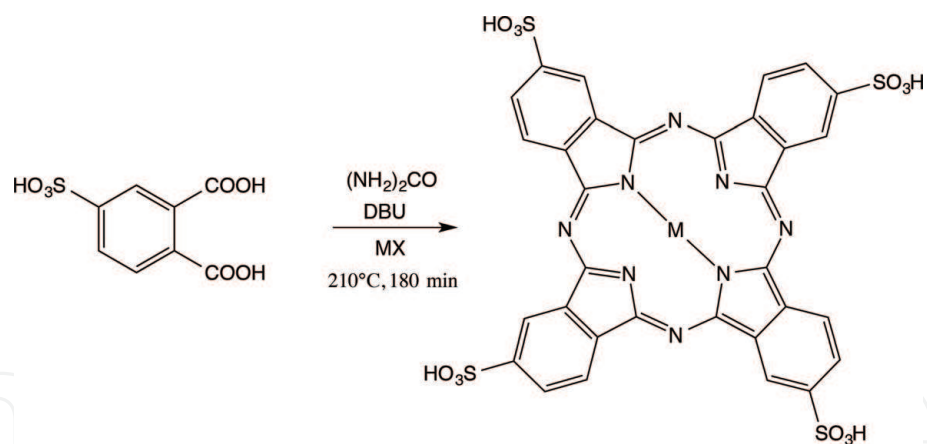
Figure 3.
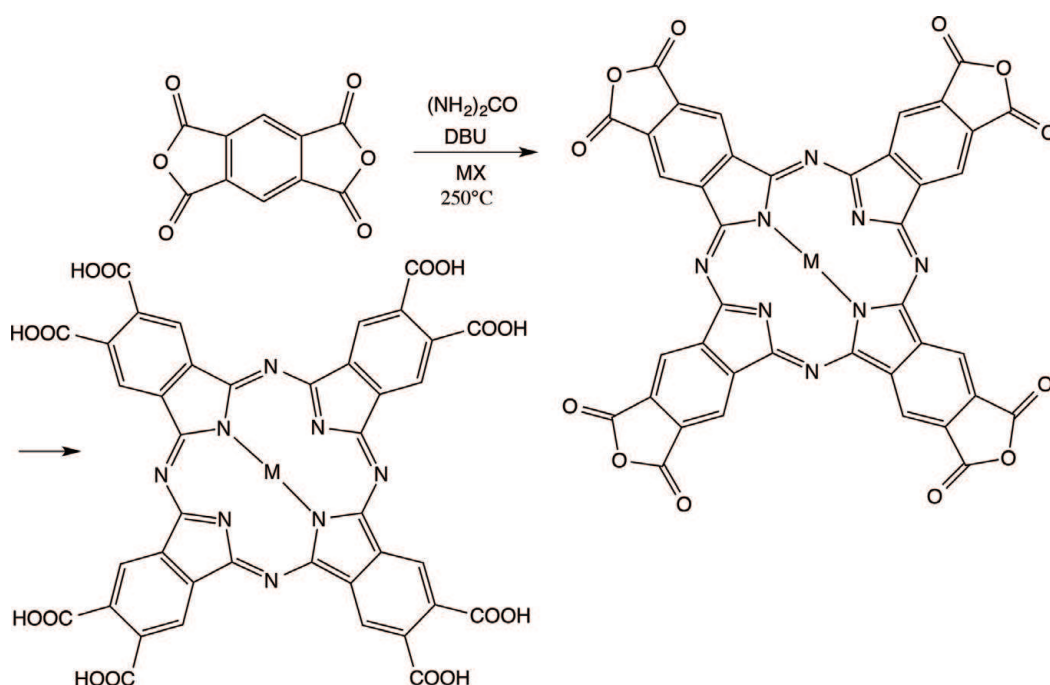*Synthetic pathway of phthalocyanine-4,4′,4 4 -tetrasulfonic acids.*

Figure 4.
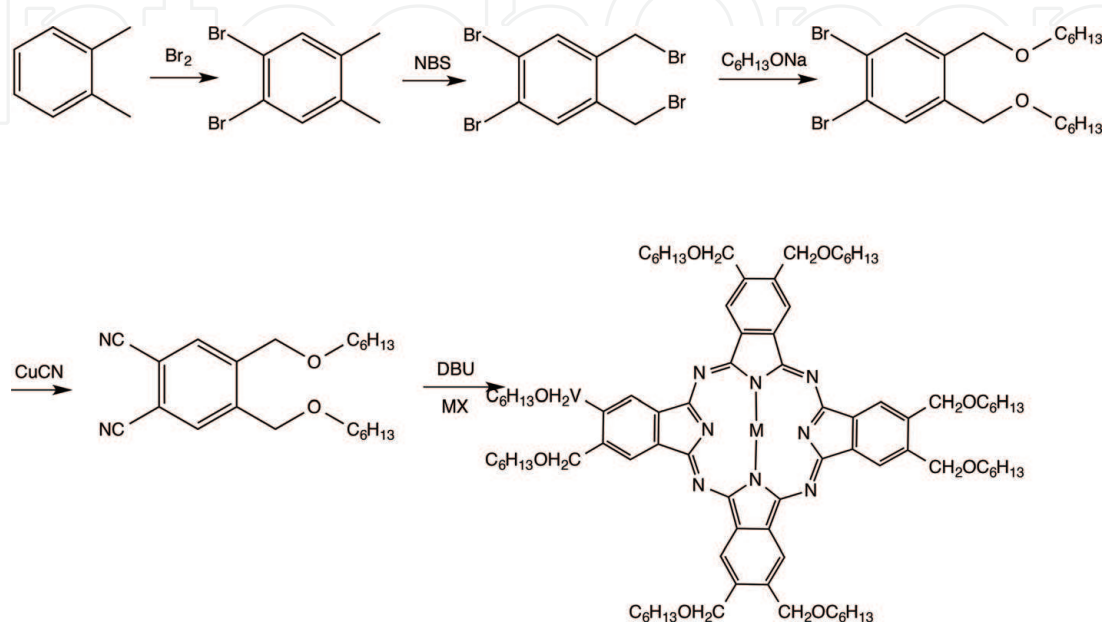*Synthetic pathway of phthalocyanine-2,3,9,10,16,17,23,24-octacarboxylic acids.*

Figure 5.
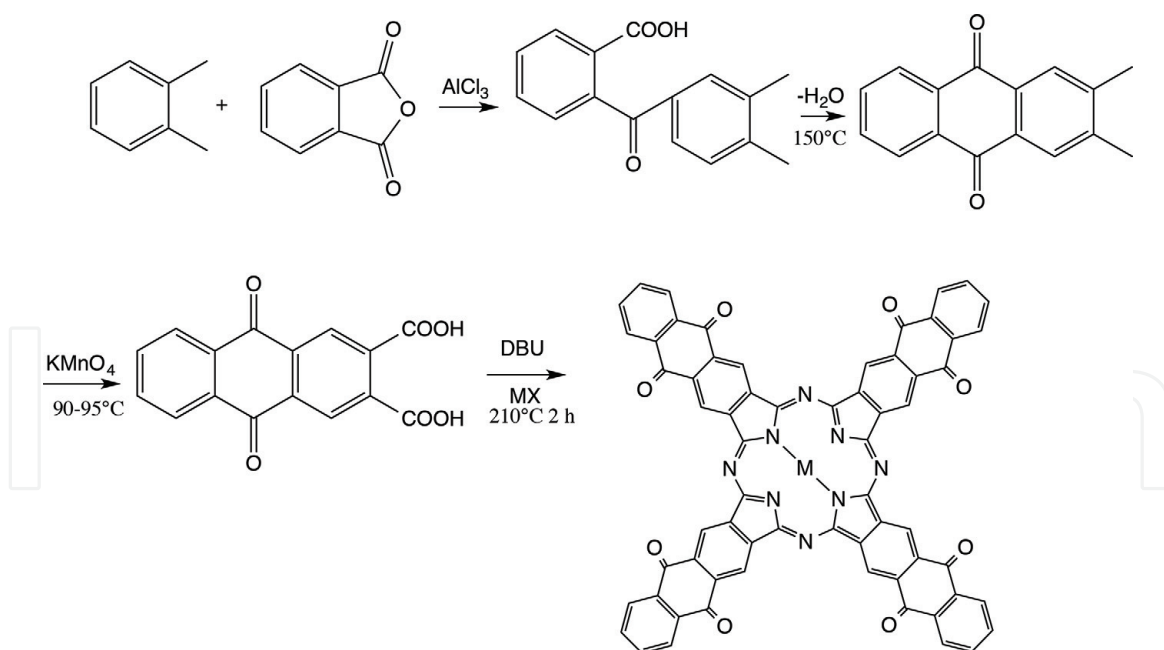*Synthetic pathway of octakis(hexoxymetyl)phthalocyanines.*

Figure 6.
Synthetic pathway of anthraquinone cyanines.

o-xylene *via* 1,2-dibromo-4,5-dimethylbenzene, 1,2-dibrom-4,5-bis(bromomethyl)benzene, and 1,2-dibromo-4,5-bis(hexoxymethyl)benzene [10] (**Figure 5**).

Anthraquinocyanines were synthesized from 9,10-anthraquinone-2,3-dicarboxylic acid, which was prepared from phthalic anhydride *via* o-(3,4-dimethylbenzoil)benzoic acid and 2,3-dimethyl-9,10-anthraquinone [10] (**Figure 6**).

These phthalocyanines have been measured by cyclic voltammograms (CVs) and chronocoulometric analysis in order to estimate their electron transfer properties and corresponding mechanism.

2.2 Synthesized nonperipheral-substituted phthalocyanines

The author also prepared nonperipheral-substituted phthalocyanine, alkylbenzo-pyridoporphyrazines, which is synthesized by reaction of 3,6-didecylphthalonitrile
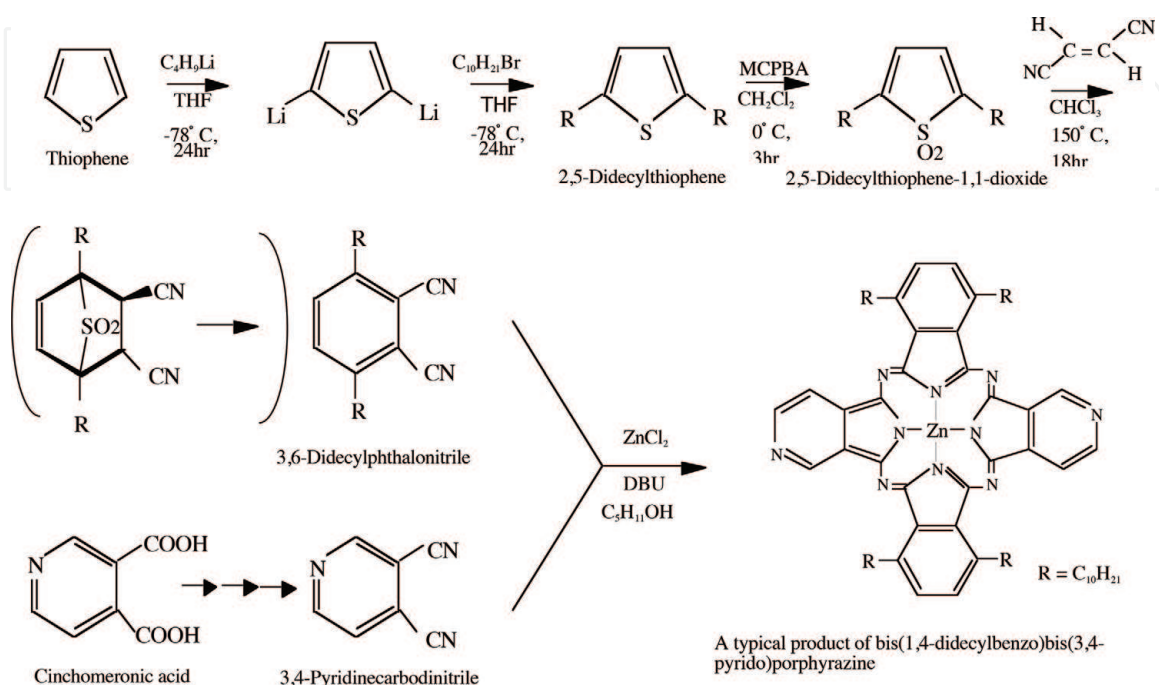

Figure 7.
Synthetic pathway of bis(1,4-didecylbenzo)-bis(3,4-pyrido)porphyrazine.

and 3,4-dicyanopyridine or 2,3-dicyanopyridine in mole ratio of 4:0, 3:1. 1:1, 1:3, and 0:4, respectively. The cross cyclotetramerization product synthesized in mole ratio of 1:1 has been separated with particular attention to give the isolation of regioisomers [17]. Intermediately, 3,6-didecylphthalonitrile was synthesized from thiophene *via* 2,5-didecylthiophene and 2,5-didecylthiophene-1,1-dioxide in accordance with our previous reports [17, 28]. The other intermediates, 3,4-dicyanopyridine and 2,3-dicyanoepyridine were prepared from cinchomeronic acid and quinolinic acid, respectively [17, 27]. The 1:1 mole ratio cross cyclotetramerization products, bis (1,4-didecylbenzo)-bis(3,4-pyrido)porphyrazine and bis(1,4-didecylbenzo)-bis (2,3-pyrido)porphyrazine, were reacted with quaternizing agents such as monochloroacetic acid, diethyl sulfate, and dimethyl sulfate in *N,N,*-dimethyl-formamide as a solvent at 140°C. After quaternation, all compounds gave the water solubility, and got amphiphilic property (**Figures 7–9**).

Nonperipheral arylsulfanyl-substituted phthalocyanines were synthesized in three steps *via* phthalonitrile-3,6-ditriflate and 3,6-bis(arylsulfanyl)phthalonitrile [19, 20, 29–31]. Intermediately, 3,6-bis(arylsulfanyl)phthalonitrile was synthesized from 2,3-dicyanohydroquinone and trifluoromethanesulfonic anhydride for 24 h. Nonperipheral arylsulfanyl phthalocyanines were synthesized from corresponding
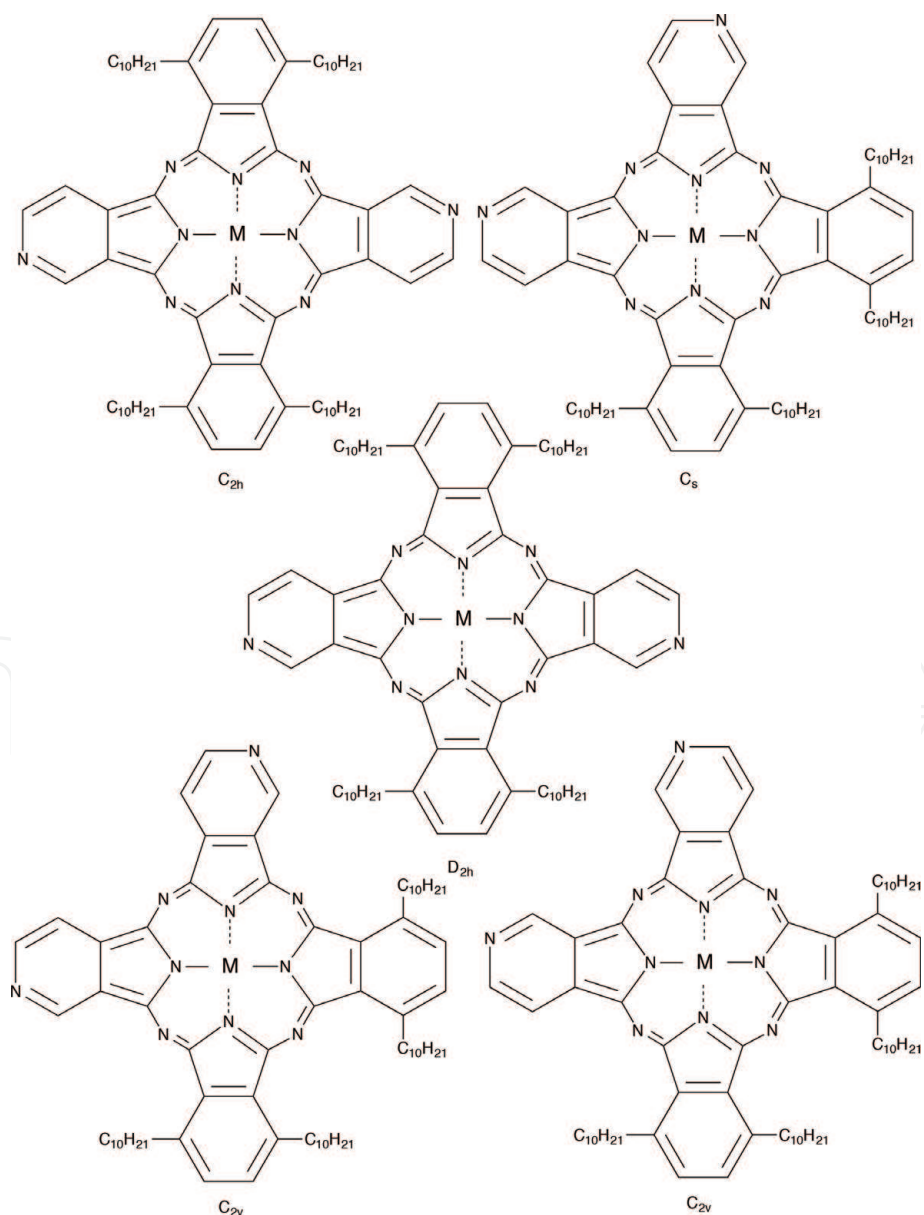

Figure 8.
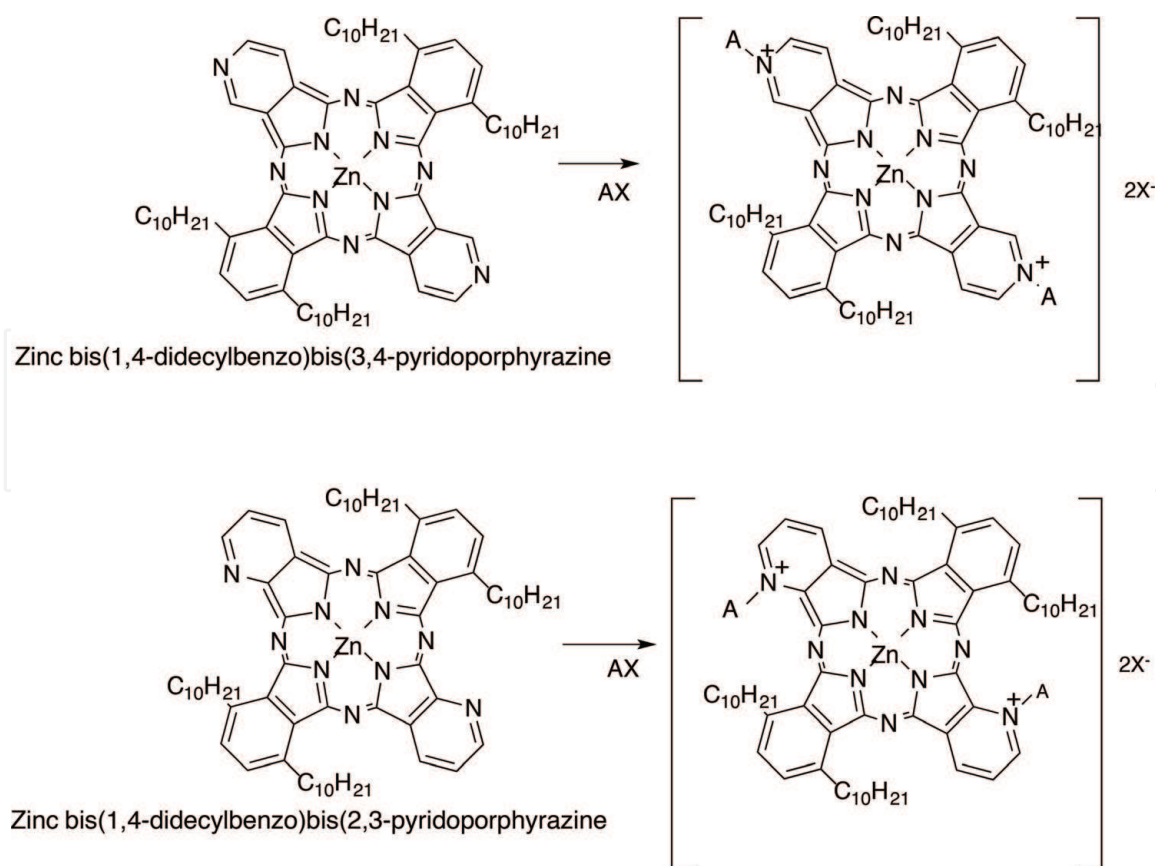*Regioisomers of metal bis(1,4-didecylbenzo)bis(3,4-pyrido)porphyrazine.*

Figure 9.
Quaternation of zinc bis(1,4-didecylbenzo)bis(3,4-pyrido)porphyrazine and zinc bis(1,4-didecylbenzo) bis(2,3-pyrido)porphyrazine; Reagents and conditions: (i) anhydrous ZnCl₂, DBU, C₅H₁₁OH, 4 h; (ii) AX: monochloroacetic acid, diethyl sulfate or dimethyl sulfate), DMF, 140°C, 2 h.
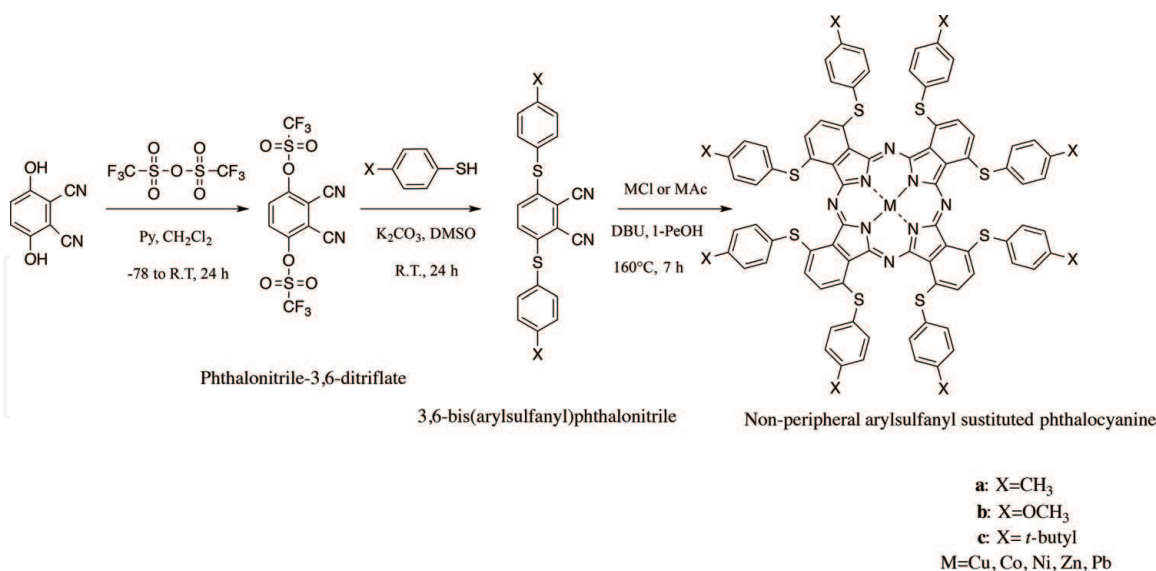

Figure 10.
Synthetic pathway of nonperipheral arylsulfanyl-substituted phthalocyanines.

3,6-bis(arylsulfanyl)phthalonitriles and metal salt in the presence of DBU as a catalyst in 1-pentanol [19, 30, 31] (**Figure 10**).

2.3 Synthesized subphthalocyanines

Subphthalocyanne is the lowest homologous compound of phthalocyanine, which consists of three isoindole units and central boron. Subphthalocyanines have

previously been used as reagents for ring enlargement reactions leading to asymmetric phthalocyanines [32] (**Figure 11**).

Subphthalocyanine and four derivatives were synthesized from 1,2-dicyanobenzene or corresponding 1,2-dicyanobenzene derivatives with boron trichloride in 1-chloronaphthalene under argon atmosphere at −3°C [33] (**Figure 12**).

Nonperipheral arylsulfanyl-substituted subphthalocyanines were also synthesized *via* phthalonitrile-3,6-ditriflate and 3,6-bis(arylsulfanyl)phthalonitrile (**Figure 13**) [34].
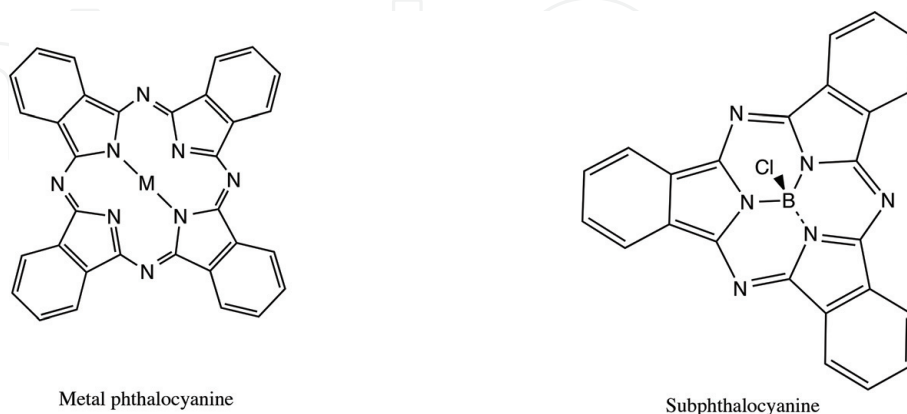

Metal phthalocyanine   Subphthalocyanine

Figure 11.
Molecular structures of metal phthalocyanine and subphthalocyanine.

a: Subphthalocyanine: R_1=H, R_2=H,
b: *Tert*-butylsubphthalocyanine: R_1= t*ert*-butyl, R_1=H, R_2=H,
c: Subphthalocyanine(S-phenyl)F_{12}: R_1=F, R_2=F,
d: Subphthalocyanine(S-phenyl)$_6F_6$: R_1=F, R_2=S-butyl,
e: Subphthalocyanine(S-butyl)$_{12}$: R_1=R_2=S-butyl,
f: Subphthalocyanine(S-phenyl)$_6F_6$: R_1=F, R_2=S-phenyl,
g: Subphthalocyanine(S-phenyl)$_{12}$: R_1=R_2=S-phenyl,

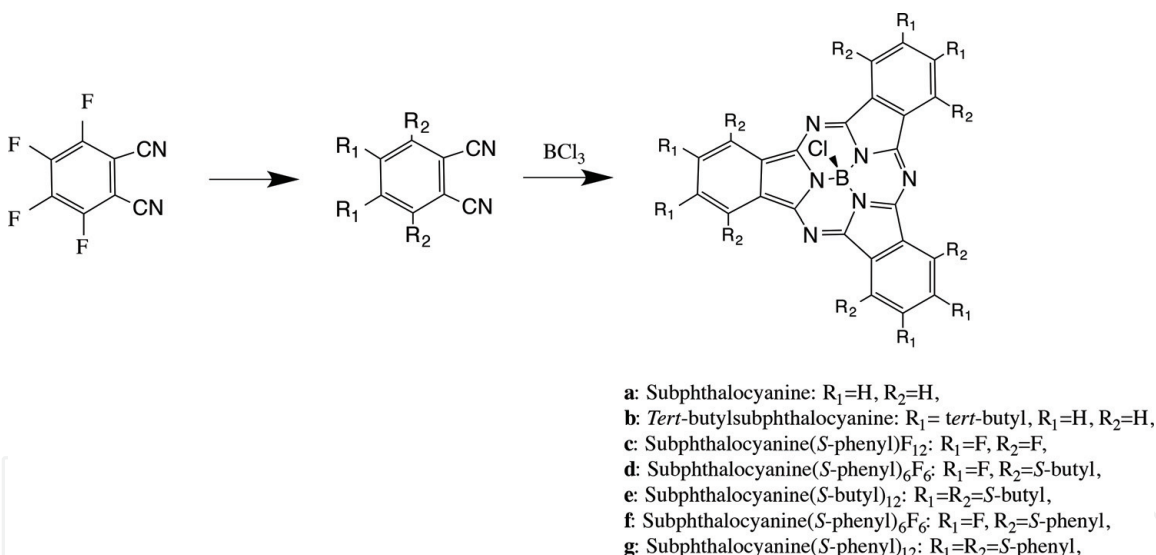**Figure 12.**
Synthetic pathway of subphthalocyanine and its six derivatives.

Non-peripheral arylsulfanyl substituted
subphthalocyanine
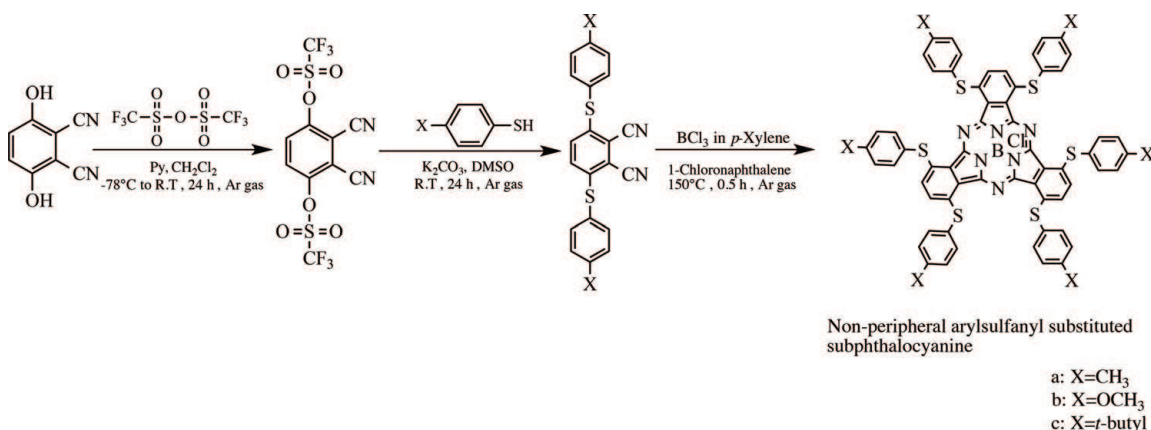
a: X=CH$_3$
b: X=OCH$_3$
c: X=*t*-butyl

Figure 13.
Synthetic pathway of nonperipheral arylsulfanyl-substituted subphthalocyanines.
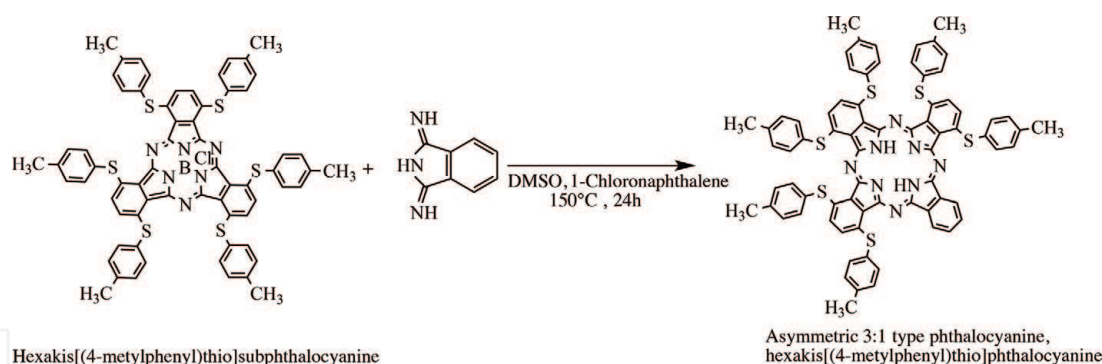
Figure 14.
Ring expansion reaction pathway to prepare asymmetric 3:1 phthalocyanine, hexakis[(4-methylphenyl)thio] phthalocyanine from hexakis[(4-methylphenyl)thio]subphthalocyanine.

To prepare asymmetric 3:1 type phthalocyanines, arylsulfanyl-subphthalocyanines and isoindoline were reacted to obtain metal-free corresponding phthalocyanines (**Figure 14**) [34].

3. Electrochemistry

3.1 Phthalocyanine-4,4′,4″4‴-tetrasulfonic acids and phthalocyanine-2,3,9,10,16,17,23,24-octacarboxylic acids, octakis(hexoxymethyl) phthalocyanine and anthraquinocyanine

CV is used in the estimation of electrochemistry. It is the electrochemical equivalent to spectroscopy. It is a useful tool for the characterization of reduction and oxidation systems. It consists of cyclic potential of a stationary electrode immersed in a quiescent solution and measuring the resulting current. The excitation signal is a linear potential scan with a triangular waveform. This triangular potential excitation signal sweeps the potential of the working electrode. The triangle returns at the same speed and permits the display of a compete voltammogram. Therefore, if a molecular is reduced in the forward scan, it will be re-oxidized on the reverse scan.
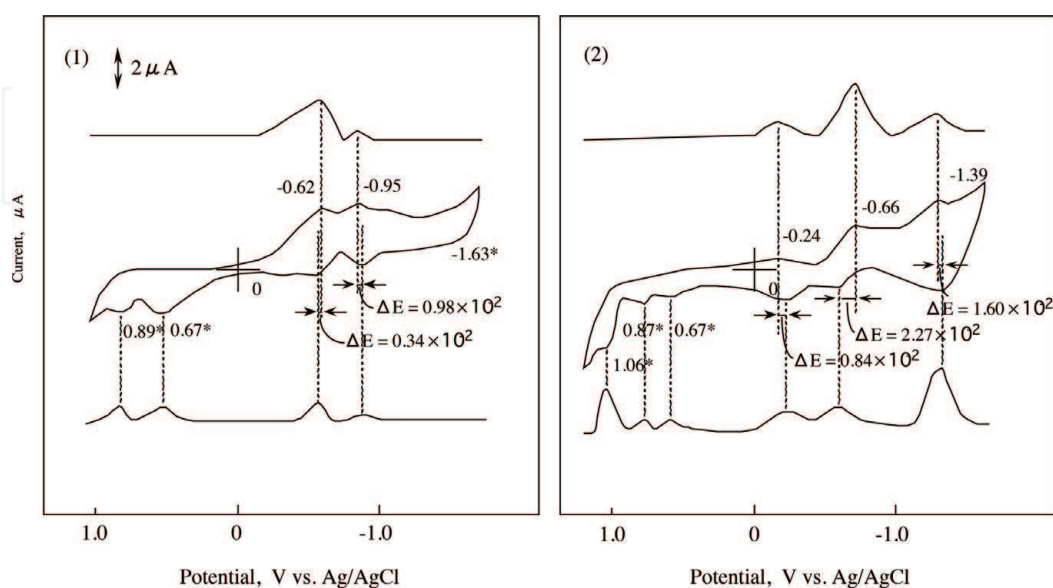

Figure 15.
*Cyclic voltammograms and their first differential curves in in dimethyl sulfoxide with 0.1 mol cm^{-3} tetrabutylammonium perchlorate, scan rate 50 mV s^{-1}. Potentials of the reversible wave are midpoint potential of anodic and cathodic peaks for each couple, $E_{1/2}$; *, irreversible peak; ΔE, the separation between the anodic and cathodic peaks for reversible couple. (1) cobalt phthalocyanine-4,4′,4 ,4 -tetrasulfonic acids, (2) cobalt phthalocyanine-2,3,9,10, 16, 17,23,24-octacarboxylic acids.*

The CV value is the current response, which depends on the applied potential. The current response shows two kinds of peaks such as the upward cathodic and the downward anodic peaks.

Cobalt phthalocyanine-4,4′,4″4‴-tetrasulfonic acids and cobalt phthalocyanine-2,3,9,10,16,17,23,24-octacarboxylic acids are measured electrochemical properties using CV and the first differential curve.

The reported potentials are the midpoint potential of anodic and cathodic peaks for each couple, $E_{1/2}$, and the peak potential for the irreversible step, which have a mark on superscript. The ΔE values are an anodic peak to cathodic peak separation located in the reduction (negative) potential region (**Figure 15**).

The CV of cobalt phthalocyanine-4,4′,4″4‴-tetrasulfonic acids showed two cathodic peaks and four anodic peaks. The peaks are attributed to four reduction stages. The first oxidation potential appeared at 0.67 V versus silver/silver chloride (Ag/AgCl) and the first reversible reduction potential at −0.62 V versus Ag/AgCl. The CV was sorted into five waves. The CVs consist of two reversible reduction couple, one irreversible reduction wave and two irreversible oxidation waves.

The CV of cobalt phthalocyanine-2,3,9,10,16,17,23,24-octacarboxylic acids, three cathodic, and six anodic peaks appeared. The peaks were sorted into three reversible reduction couples at −0.24, −0.66, and −1.39 V versus Ag/AgCl, and three irreversible oxidation waves at 0.67, 0.87, and 1.06 V versus Ag/AgCl. The reduction and oxidation of metal phthalocyanines are due to the interaction between the phthalocyanine macro-ring and the central metal. Sulfonic and carboxylic groups are electron-withdrawing groups, so they are expected to reduce the electro charge in the phthalocyanine macro-ring.

The CV of cobalt 2,3,9,10,16,17,23,24-octakis(hexoxymethyl)phthalocyanine showed four cathodic peaks at 0.16, −0.49, −0.73, and −1.54 V versus Ag/AgCl, and three anodic peaks at 0.73, −0.61, and −1.47 V versus Ag/AgCl. The CV of cobalt 2,3,9,10,16,17,23,24-octakis(hexoxymethyl)phthalocyanine was sorted into two irreversible oxidation waves at 0.16 and 0.73 V versus Ag/AgCl, and two pare of reversible potential. The negative charge is expected to increase on the phthalocyanine macro-ring, since the substituent hexoxymethyl is the electro-donating group.

The CV of cobalt anthraquinocyanine showed a solitary shape in comparison with the other cobalt phthalocyanine-4,4′,4″4‴-tetrasulfonic acids, cobalt phthalocyanine-2,3,9,10,16,17,23,24-octacarboxylic acids, and cobalt 2,3,9,10,16,17,23,24-octakis(hexoxymethyl)phthalocyanine. The shape of CV for cobalt anthraquinocyanine was sorted into three cathodic peaks at 0.19, −0.69, and −0.95 V versus Ag/AgCl, and two anodic peaks at 0.87 and −0.58 V versus Ag/AgCl. Cobalt anthraquinocyanine has almost one pair of reversible potential.

The relationship between the anodic and cathodic peak current ratio of a reversible couple, i_a/i_c and the scan rate, v, provides a quick test for electrochemical mechanism associated with a preceding or succeeding reversible or irreversible chemical equilibrium. The scan rate varied from 0.05 to 0.3 Vs^{-1} (**Figure 16**).

The ratio of i_a/i_c decreased with an increased v, all reversible couples of cobalt phthalocyanine-4,4′,4″4‴-tetrasulfonic acids, cobalt phthalocyanine-2,3,9,10,16,17,23,24-octacarboxylic acids, cobalt 2,3,9,10,16,17,23,24-octakis(hexoxymethyl)phthalocyanine, and cobalt anthraquinocyanine. The reversible reduction couples of cobalt phthalocyanine-4,4′,4″4‴-tetrasulfonic acids, cobalt phthalocyanine-2,3,9,10,16,17,23,24-octacarboxylic acids, cobalt 2,3,9,10,16,17,23,24-octakis(hexoxymethyl)phthalocyanine, and cobalt anthraquinocyanine are characterized as a fast reversible electron transfer followed by a reversible chemical reaction. The values of i_a/i_c converge extrapolated to zero of v, the third reduction potential of cobalt phthalocyanine-2,3,9,10,16,17,23,24-octacarboxylic acids.
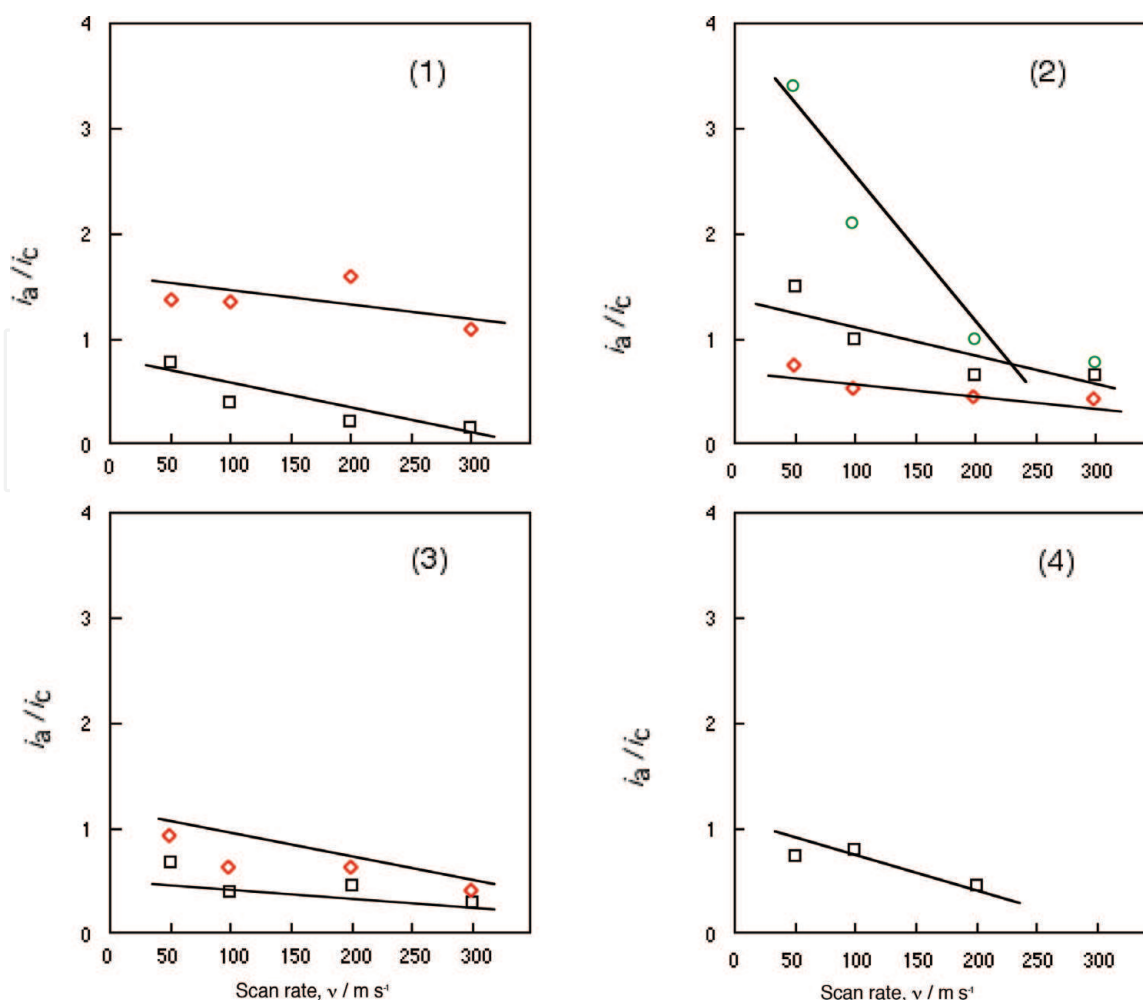
Figure 16.
Change in the anodic to cathodic current ratio with scan rate v. (1) cobalt phthalocyanine-4,4',4',4 -tetrasulfonic acids; (2) cobalt phthalocyanine-2,3,9,10,16,17,23,24-octacarboxylic acids; (3) cobalt octakis (hexoxymethyl)phtalocyanine; (4) cobalt anthraquinocyanine. Square: first redox couple; Diamond: second redox couple; Circle: third redox couple.

The potentials of ΔE are around 100 mV, except for cobalt phthalocyanine-2,3,9,10,16,17,23,24-octacarboxylic acids. Extrapolated to zero of v, the ΔE values approach close to 60 mV. The electrode process of cobalt phthalocyanine-4,4',4''4'''-tetrasulfonic acids, cobalt phthalocyanine-2,3,9,10,16,17,23,24-octacarboxylic acids, cobalt 2,3,9,10,16,17,23,24-octakis(hexoxymethyl)phthalocyanine, and cobalt anthraquinocyanine take place almost one-electron transfer. The $E_{1/2}$ is independent of v and has constant value. These electrode processes are diffusion-controlled complicated electron transfer having some weak absorption with the oxide (**Table 1**).

Chronoamperometry is a current-time response to a potential step excitation signal. A large cathodic current flows immediately when the potential is stepped up from the initial value, after that it slowly attenuates. The reduction step exhibited that same behavior in comparison with both potential steps. The current-time curves are converted into the relation between the current and square root of time $t^{1/2}$ (**Figures 17** and **18**).

The current-time curve for chronoamperometry is expressed by the Cottrell equation (Eq. (1)).

$$i = \frac{nFCD^{1/2}}{\pi^{1/2}t^{1/2}} = Kt^{1/2} \qquad (1)$$

where i is the current (A), n is the number of electrons transferred per ion or molecule (mol^{-1}), F is Faraday's constant (96,485 C mol^{-1}), A is the electrode

Compounds	Potential / V *vs.* Ag/AgCl						
	Reduction				Oxidation		
Cobalt phthalocyanine-4,4',4",4"'-tetrasulfonic acids	-1.63*	-0.95	-0.62		0.67*	0.89*	
ΔE**	0.98		0.34				
Cobalt phthalocyanine-2,3,9,19,16,17,23,24-octacarboxylic acids	-1.39		-0.66	-0.24	0.67*	0.89*	1.06*
ΔE**	1.6		2.27	0.84			
Cobalt octakis(hexoxymethel)phthalocyanine	-1.50	-1.25*	-0.67	-0.49*	0.16*	0.73*	
ΔE**	0.88		1.27				
Cobalt anthaquinocyanine	-0.95*	-0.63			0.19*	0.87*	
ΔE**	1.07						

Potentials of reversible wave are midpoint potential of anodic and cathodic peaks for each couple, $E_{1/2}$.

* Irreversible peak.

** The anodic peak to cathodic peal separation of reversible couple.

Table 1.
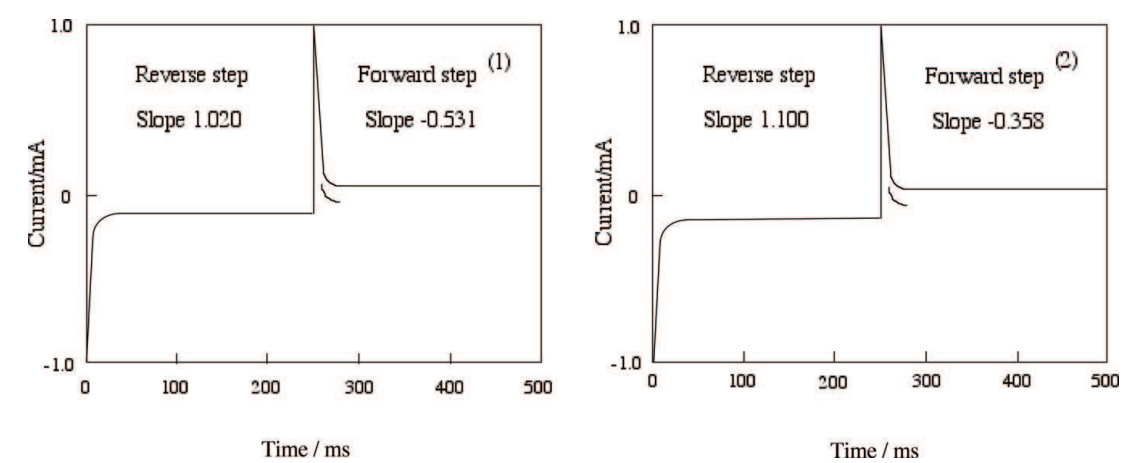*Reduction and oxidation potentials.*

Figure 17.
Chronoamperometry and the slope calculated from the Cottrell plot. Potential step; −1.2 to 1.6 V versus Ag/AgCl, time interval: 250 ms. (1) Cobalt phthalocyanine-4,4',4 ,4 -tetrasulfonic acids. (2) Cobalt phthalocyanine-2,3,9,10,16,17,23,24-octacarboxylic acids.
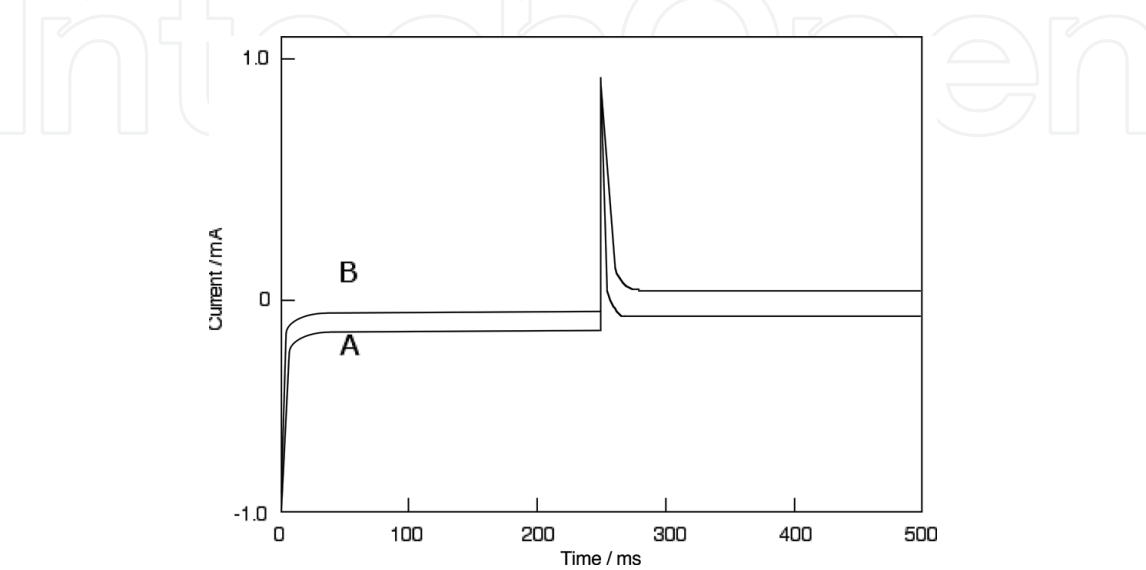

Figure 18.
Chronoamperometry of cobalt oktakis(hxoxymethyl)phthalocyanine. A: pulse step −1.2 to 0 V versus Ag/AgCl, step width 250 ms. B: pulse step −1.2 to 1.6 V versus Ag/AgCl, step width 250 ms.

area ($2.0 \cdot 10^{-2}$ cm^2), C is the concentration (mol cm^{-3}), D is the diffusion constant (cm s^{-1}), and t is time (s). A plot of the current, i versus square root of time, $t^{1/2}$ gives a straight line. The slop means the diffusion constant in forward and reverse steps.

Electron processes in the systems are diffusion-controlled electron transfers mentioned above. Relationships between i and $t^{1/2}$ are considered to be a finite diffusion for cobalt phthalocyanine-4,4′,4″4‴-tetrasulfonic acids and cobalt phthalocyanine-2,3,9,10,16,17,23,24-octacarboxylic acids.

The current of the Cottrell plots is a measure of the rate for electrolysis at the electrode surface. Electrolysis is controlled with a mass transfer by diffusion on the electrode. The diffusion constant implies the rate of electrolysis. The slop means the diffusion constant in each step. The forward step indicates the reduction and the reverse step is oxidation (**Table 2**).

The chronocoulometry was taken by one treatment of chronoamperometry. The current response was integrated to give a response to the charge. The charge-time curve of the forward step for chronocoulometry is the integral of Eq. (1); this is called the Anson equation (Eq. (2)).

$$Q = \frac{2nFACD^{1/2}t^{1/2}}{\pi^{1/2}} = 2Kt^{1/2} \tag{2}$$

The reverse step is following equation (Eq. (3)):

$$Qr = \frac{2nFACD^{1/2}}{\pi^{1/2}} \left\{ \tau^{1/2} + (1-r)^{1/2} - t^{1/2} \right\} \tag{3}$$

where τ is time of reverse potential step.

The initial potential was -1.20 V versus Ag/AgCl and the step width was 250 ms. The step potential was 1.60 V versus Ag/AgCl (**Figure 19**).

For cobalt phthalocyanine-4,4′,4″4‴-tetrasulfonic acids, cobalt phthalocyanine-2,3,9,10,16,17,23,24-octacarboxylic acids, cobalt 2,3,9,10,16,17,23,24-octakis (hexoxymethyl)phthalocyanine, and cobalt anthraquinocyanine, the extent of diffusion control increases systematically as the standard potential becomes positive. In the forward step, the electron change reached at about 30 μC. Then, the electron change was decreased 15 μC, except for cobalt phthalocyanine-2,3,9,10,16,17,23,24-octacarboxylic acids. The reverse step was attenuated to 0 μC with 70 ms in the chronocoulometry of the reduction side from -1.20 to 0.00 V versus Ag/AgCl potential, except for cobalt phthalocyanine-2,3,9,10,16,17,23,24-octacarboxylic acids. The chronocoulometry had a linear forward step and a flat reverse step indicating no Faradic activity for all compounds in the oxidation side from the 0.00 to 1.60 V versus Ag/AgCl step.

Compound	Forward step / mV		Reverse step /mV	
	Slop	Intercept	Slop	Intercept
Cobalt phthalocyanine-4,4',4",4'''-tetrasulfonic acids	-0.531	-0.0631	1.020	0.00596
Cobalt phthalocyanine-2,3,9,10,16,17,23,24-octacarboxylic acids	-0.358	-0.1060	1.100	-0.00274
Cobalt octakis(hexoxymethyl)phthalocyanine	-0.525	-0.0360	0.670	-0.000172
Coblt anthraquinocyanine	-0.322	-0.0632	0.698	0.00547

Table 2.
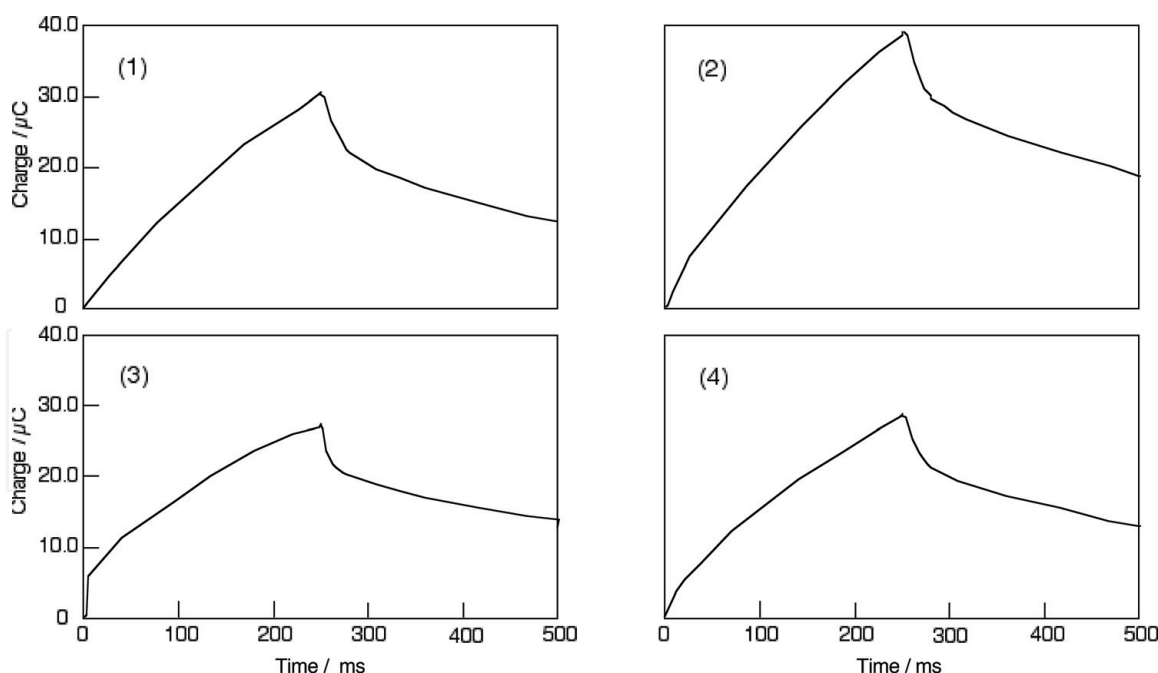*The slop and intercept of the Cottrell plot.*

Figure 19.
Chronocoulometry of (1) cobalt phthalocyanine-4,4',4,4-tetrasulfonic acids, (2) cobalt phthalocyanine-2,3,9,10,16,17,23,24-octacarboxylic acids, (3) cobalt octakis(hexoxymethyl)phthalocyanine, (4) cobalt anthraquinocyanine. Potential step: −1.2 to 1.6 V versus Ag/AgCl, step width 250 ms.

The Anson plots are converted from the charge-time curve of chronocoulometry into the relation between charge and $t^{1/2}$ (**Figure 20**).

The Anson plot is a straight line with an intercept. Chronocoulometry is useful to study absorption on an electrode surface. When absorbed species exist on an electrode surface, it is electrolyzed immediately, whereas solution species must diffuse the electrode in order to react. The total charge Q_{total} is measured in a potential step experiment.

$$Q_{total} = \frac{2nFACD^{1/2}}{\pi^{1/2}} + Q_{dl} + Q_{abs} \tag{4}$$

$$Q_{abs} = nFA\Gamma \tag{5}$$

where Q_{dl} is the double layer charge (C), Q_{abs} is the absorbed species charge (C), Γ is the amount absorbed (mol cm^{-3}). Q_{total} is obtained by summing Q, Q_{abs}, and Q_{dl}. As the expression of Q in Eq. (2), a plot of Q versus $t^{1/2}$ is a straight line. The
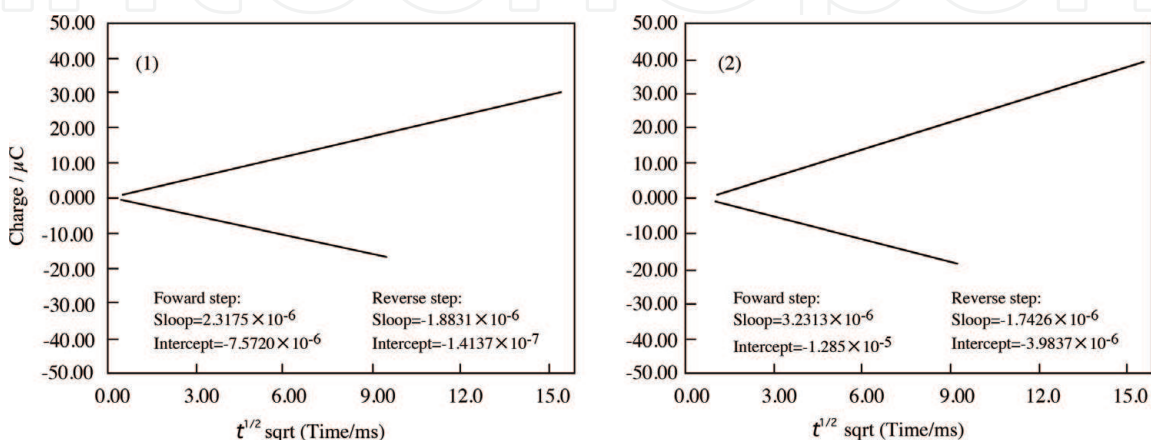

Figure 20.
Anson plots of (1) cobalt phthalocyanine-4,4',4,4-tetrasulfonic acids and (2) cobalt phthalocyanine-2,3,9,10,16,17,23,24-octacarboxylic acids.

Anson plot should be linear with intercept that is equal to the second and third terms in Eq. (4). If Q_{dl} is known, then, the value Q_{abs} can be calculated for an electrode of the known electrode area. When double step chronocoulometry is used, the difference in the intercepts of forward and reverse steps is Q_{abs}.

Only the value of Q in three terms depends upon the scanning time. The intercept of the Anson plot expresses the sum of Q_{dl} and Q_{abs}. The Q_{abs} can take away Q_{dl}, which is a value of the difference of intercepts between forward and reverse steps, since double step chronocoulometry is used. When no absorption of reactant or product, the intercept of Anson plot for both forward and reverse steps are equal (Q_{dl}). While reactant absorbs but product does not, the intercept of reverse is a measure of Q_{dl} in the presence of absorbed reactant, and the intercept of forward step contains both Q_{dl} and Q_{abs} for absorbed reactant.

The chronocoulometry of cobalt phthalocyanine-4,4′,4″4‴-tetrasulfonic acids, cobalt phthalocyanine-2,3,9,10,16,17,23,24-octacarboxylic acids, cobalt 2,3,9,10,16,17,23,24-octakis(hexoxymethyl)phthalocyanine, and cobalt anthraquinocyanine shows that the reactant is absorbed but not the product. In regard to the absorption using Eqs. (2) and (3), the Q_{abs} calculated to 7.40, 8.92, 2.81, and 7.07 μC for cobalt phthalocyanine-4,4′,4″4‴-tetrasulfonic acids, cobalt phthalocyanine-2,3,9,10,16,17,23,24-octacarboxylic acids, cobalt 2,3,9,10,16,17,23,24-octakis(hexoxymethyl)phthalocyanine, and cobalt anthraquinocyanine, respectively.

The relation between Q_r/Q_f and $t^{1/2}$ can be estimated by the mechanism and rate of the following chemical reaction (**Figure 21**).

The value Q_r/Q_f indicates the base line for the chronocoulometry of the reverse step charge Q_r divided by the final value of forward step Q_f. This relationship can be estimated by the mechanism and rate of following reaction. The following chemical reaction obeyed first-order kinetics, which found the calculation to be 0.20, 0.26, 0.30, and 0.30 s^{-1} for cobalt phthalocyanine-4,4′,4″4‴-tetrasulfonic acids, cobalt phthalocyanine-2,3,9,10,16,17,23,24-octacarboxylic acids, cobalt 2,3,9,10,16,17,23,24-octakis(hexoxymethyl)phthalocyanine, and cobalt anthraquinocyanine [10, 26, 27].

The oxidation of metal phthalocyanines having transition metal are electrochemically irreversible and electrons are added to the orbital of phthalocyanine ring or the central metal depending on the redox potential for reduction process.
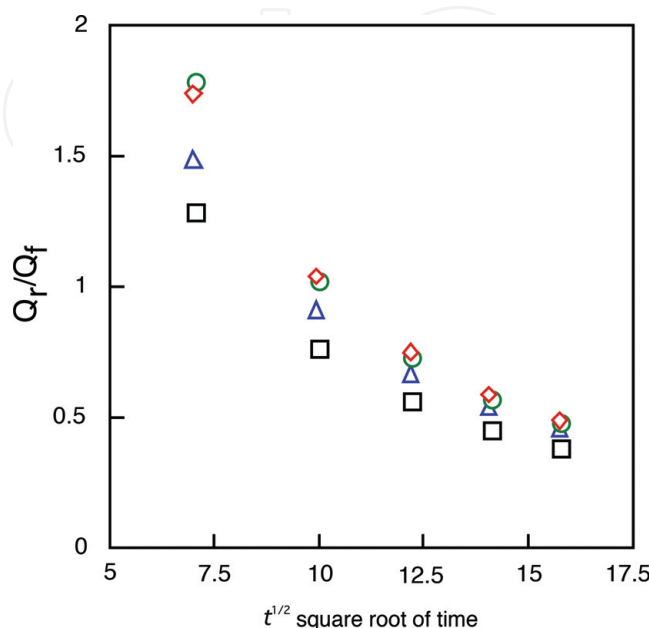

Figure 21.
Variation of Q_r/Q_f with square root of time, $t^{1/2}$ for cobalt anthraquinocyanine.

3.2 Nonperipheral alkylbenzopyridoporphyrazines and nonperipheral arylsulfanyl substituted phthalocyanines

Nonperipheral alkylbenzoporphyrazines synthesized by reaction of 3,6-didecylphthalonitrile and 3,4-dicyanopyridine or 2,3-dicyanopyridine in mole ratio of 4:0, 3:1. 1:1, 1:3, 0:4, respectively. The 1:1 mole ratio cross cyclotetramerization product has been separated with particular attention given to the isolation of regioisomers [17]. At the first time, 3,6-didecylphthalonitrile and 3,4-dicyanopyridine have been reacted together in ratio of 1:1 product, zinc bis (1,4-didecylbenzo)-bis(3,4-pyrido)porphyrazine. The zinc bis(1,4-didecylbenzo)-bis(3,4-pyrido)porphyrazine has two nonperipheral-substituted benzenoido and pyridinoido rings, which are in different locations. The CV can be used to make an estimation of the electrochemical difference for regioisomers (**Table 3**).

Before separation of regioisomers, the reduction and oxidation potentials of zinc bis (1,4-didecylbenzo)-bis(3,4-pyrido)porphyrazine are sorted into six irreversible peaks.

After separation of regioisomers, fractions 1–3 have one pair of reversible oxidation peak and four irreversible waves. Fraction 4 has one pair of reversible and three irreversible waves.

The porphyrazine ring is influenced by the π-electrons about the closed system. Although the π-electron system of zinc bis(1,4-didecylbenzo)-bis(3,4-pyrido) porphyrazine and fractions 1–4 consists of one porphyrazine, two pyridinoid, and two didecyl-substituted benzenoid rings; the location of these rings except for porphyrazine are different from each regioisomer.

Substituents and pyridonoid rings influenced the π-electron environment in zinc bis(1,4-didecylbenzo)-bis(3,4-pyrido)porphyrazine and fractions 1–4. The effect of pyridinoid rings gave rise to the change of the electron density of the metal phthalocyanines. The difference of reduction and oxidation peaks between fractions 1 and 4 is attributed to the effect of variation of the interaction between the central metal and the alkylbenzoporphyrazine. Following this, the difference in CVs between zinc bis(1,4-didecylbenzo)-bis(3,4-pyrido)porphyrazine and fractions 1–4 is also the effect of interaction, since zinc bis(1,4-didecylbenzo)-bis(3,4-pyrido)porphyrazine

Materials	Potential / V *vs.* Ag/AgCl					
	Reduction				Oxidation	
Zinc bis(1,4-didecylbenzo)-bis(3,4-pyrido)porphyrazine	-0.97*	-0.71*	-0.45*	-0.15*	0.37*	0.93*
Fraction 1 D_{2h}	-1.00*	-0.58*	-0.24*		0.44	0.93*
ΔE**					0.17	
Fraction 2 C_{2h}	-1.05*	-0.60*	-0.19*		0.37	0.90*
ΔE**					0.10	
Fraction 3 C_s	-0.96*	-0.65*	-0.22*		0.37	0.89*
ΔE**					0.13	
Fraction 4 C_{2v}	-0.87*	-0.63*	-0.21*		0.34	
ΔE**					0.01	

Zinc bis(1,4-didecylbenzo)bis(3,4-pyrido)porphyrazine was before separation of its regioisomers.
Potentials of reversible wave are midpoint potential of anodic and cathodic peaks for each couple, $E_{1/2}$.
* Irreversible peak.
** The anodic peak to cathodic peak separation for reversible.

Table 3.
Reduction and oxidation potential of zinc bis(1,4-didecylbenzo)bis(3,4-pyrido)porphyrazine and its regioisomers (fractions 1–4).

is a mixture of its regioisomers. The regioisomers of zinc bis(1,4-didecylbenzo)-bis (3,4-pyrido)porphyrazine decided the symmetry of molecular structure as D_{2h}, C_{2h}, C_s and C_{2v} for fractions 1, 2, 3 and 4, respectively. However, two types of C_{2v} isomers of zinc bis(1,4-didecylbenzo)-bis(3,4-pyrido)porphyrazine cannot be isolated.

The ΔE values are around 100 mV and the reduction and oxidation processes are the same for regioisomers, except for fraction 4. The electron process of regioisomers between fractions 1 and 3 involves approximately one electron transfer. The ΔE values of fraction 4 show different behavior in comparison to the others. The different behavior for fraction 4 is attributable to the mixture of two types of C_{2v} regioisomers. The reduction and oxidation potentials of fraction 4 are based on the interaction between two types of C_{2v} regioisomers. No observation on the reversible couple in zinc bis(1,4-didecylbenzo)-bis(3,4-pyrido)porphyrazine resulted in interaction between regioisomers.

Zinc bis(1,4-didecylbenzo)-bis(3,4-pyrido)porphyrazine and zinc bis (1,4-didecylbenzo)-bis(2,3-pyrido)porphyrazine were reacted with quaternizing agents such as monochloroacetic acid, diethyl sulfate, and dimethyl sulfate in *N, N,*-dimethylformamide. These compounds were not separated of their regioisomers [10, 17–19].

The shapes of CVs were changed between before and after the quaternation. The reduction and oxidation potentials were shown two anodic and four cathodic peaks for zinc bis(1,4-didecylbenzo)-bis(3,4-pyrido)porphyrazine, and three anodic and four cathodic waves for zinc bis(1,4-didecylbenzo)-bis(2,3-pyrido)porphyrazine (**Figure 22** and **Table 4**).

The redox potential of regioisomers of zinc bis(1,4-didecylbenzo)-bis (3,4-pyrido)porphyrazine were varied (**Table 5**).

After quaternation of regioisomers, the shapes of CVs appeared clearly. The electron transfer ability of regioisomers has been increased remarkably by the acquisition of cation groups. The CV showed two anodic and two cathodic
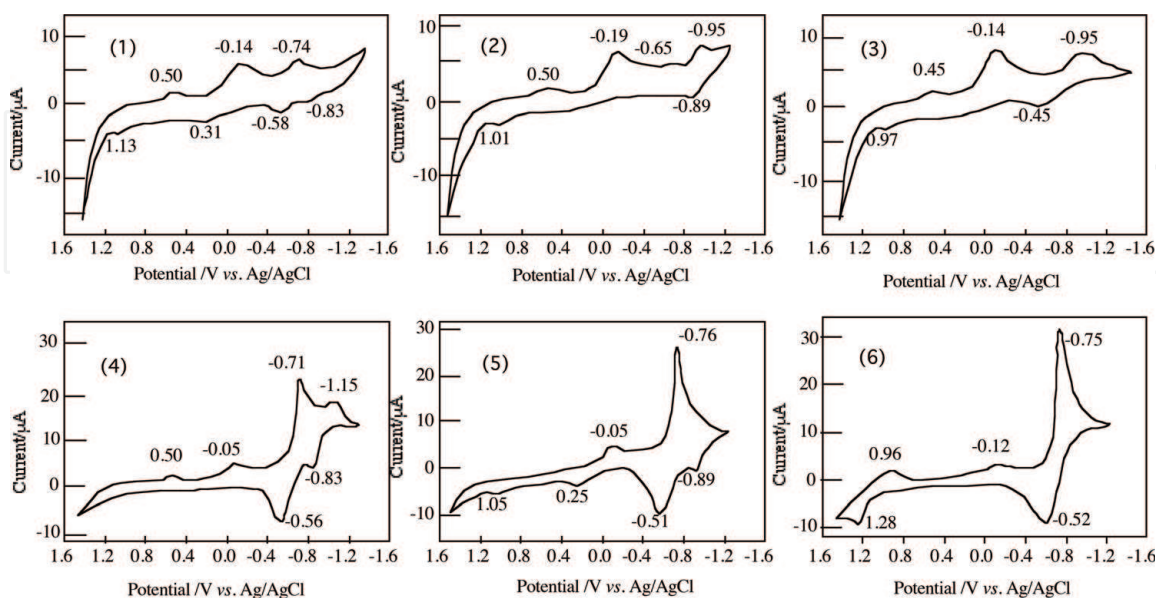

Figure 22.
Potentials of amphiphilic alkylbenzopyridoporphyrazines in N,N-dimethylformamide with tetrabutylammonium perchlorate. (1) bis(1,4-didecylbenzo)-bis(3,4-pyrido)porphyrazine react with dimethyl sulfate, (2) bis(1,4-didecylbenzo)-bis(3,4-pyrido)porphyrazine react with diethyl sulfate, (3) bis(1,4-didecylbenzo)-bis(3,4-pyrido)porphyrazine react with monochloroacetic acid, (4) bis (1,4-didecylbenzo)-bis(2,3-pyrido)porphyrazine react with dimethyl sulfate, (5) bis(1,4-didecylbenzo)-bis (2,3-pyrido)porphyrazine react with diethyl sulfate, (6) bis(1,4-didecylbenzo)-bis(2,3-pyrido)porphyrazine react with monochloroacetic acid.

Compound	Potential / V *vs.* Ag/AgCl						
	Reduction				Oxidation		
Zinc bis(1,4-didecylbenzo)-bis(pyrido)porphyrazine	-0.97*	-0.71*	-0.45*	-0.15*	0.37*	0.93*	
Quaternized with monochloroacetic acid	-0.95*	-0.45*	-0.41*		0.45*	0.97*	
Quaternized with dietyl sulfate	-0.95*	-0.89	-0.65*	-0.19*	0.50*	1.01*	
ΔE**		0.13					
Quaternized with dimethyl sulfate	-0.78	-0.58*	-0.14*		0.31	0.50*	1.13*
ΔE**		0.10					

Potential of reversible wave are midpoint potentials of anodic and cathodic peaks for each couple, $E_{1/2}$.

* Irreversible peak.

** The anodic peak to cathodic peak separation for reversible couple.

Table 4.
Reduction and oxidation potential of zinc bis(1,4-didecylbenzo)-bis (3,4-pyrido)porphyrazine and its quaternized compound with monochloroacetic acid, diethyl sulfate and dimethyl sulfate.

Compounds	Potential / V *vs.* Ag/AgCl				
	Reduction			Oxidation	
Fraction 1 D_{2h}	-0.85*	-0.24		1.02	
ΔE**		0.04			
Fraction 2 C_{2h}	-1.00*	-0.63*	-0.24*	0.47*	0.98*
ΔE**					
Fraction3 C_s	-0.79*	-0.55*	-0.15*	1.09*	
ΔE**					
Fraction 4 C_{2v}	-0.73*	-0.57	-0.31*	0.13*	0.47*
ΔE**		0.07			

Potentials of reversible wave are midpoint potential of anodic and cathodic peaks for each couple, $E_{1/2}$.

* Irreversible peak.

** The anodic peak to cathodic peak separation for reversible couple.

Table 5.
potential of separated regioisomers in zinc bis(1,4-didecylbenzo)-bis(3,4-Pyrido)porphyrazine.

peaks, two anodic and three cathodic peaks, two anodic and two cathodic peaks, and one anodic and five cathodic peaks for fractions 1, 2, 3, and 4, respectively.

The CVs of nonperipheral arylsulfanyl substituted metal-free phthalocyanines such as oxtakis[(4-methylphenyl)thio]phthalocyanine, octakis[(4-methoxyphenyl) thio]phthalocyanine, and octakis[(4-*tert*-butylphenyl)thio]phthalocyanine are of similar shape. The CVs of these metal-free phthalocyanines are known to exhibit irreversible oxidation and reduction potentials around 0.6 and −0.7 V versus the standard hydrogen electrode (SHE), respectively. The reduction and oxidation potentials of phthalocyanines appear from the interaction between the phthalocyanine ring and the central metal atom. In these metal-free phthalocyanines, the shapes of oxtakis[(4-methylphenyl)thio]phthalocyanine, octakis[(4-methoxyphenyl)thio]
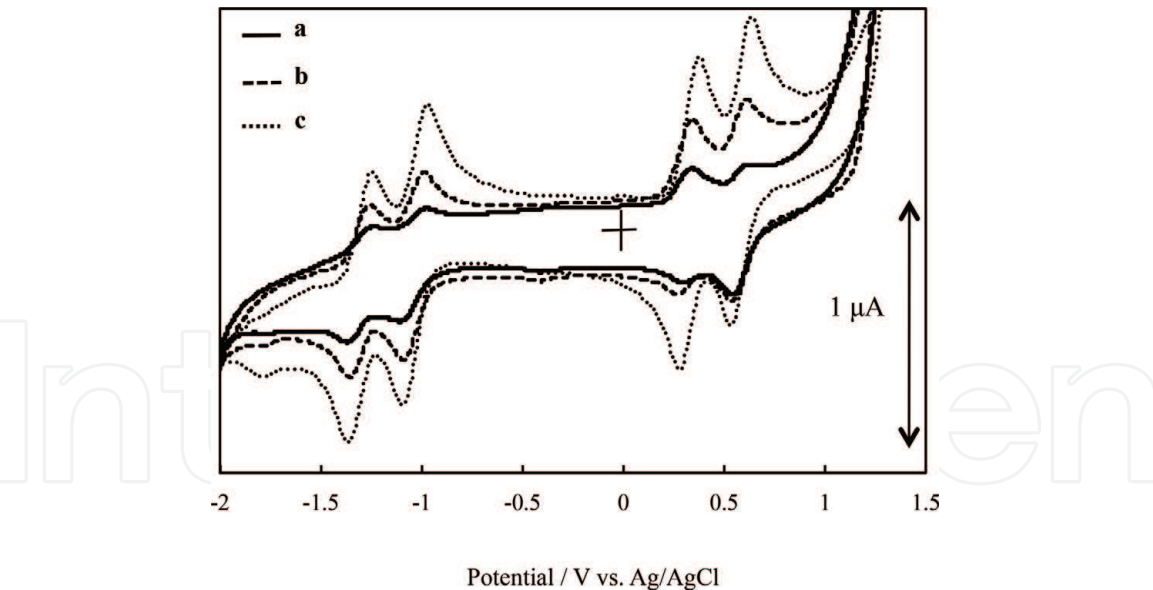
Figure 23.
Cyclic voltammograms of nonperipheral arylsulfanyl-substituted phthalocyanines in odichlorobenzene with 0.1 mol cm⁻³ tetrabutylammonium perchlorate. a: octakis[(4-methylphenyl)thio]phthalocyanine; b: octakis [(4-mthoxylphenyl)thio]phthalocyanine; c: octakis[(4-tert-butyllphenyl)thio]phthalocyanine.

phthalocyanine, and octakis[(4-*tert*-butylphenyl)thio]phthalocyanine showed four cathodic peaks and four anodic peaks. These pairs of peaks arose around −1.3, −1.05, −0.3, and 0.6 V versus Ag/AgCl (**Figure 23**).

The CVs of nonperipheral arylsulfanyl-substituted lead phthalocyanines have similar shapes unconcerned in the presence of terminal groups such as methyl, methoxy, and *tert*-butyl, on the arylsulfanyl substituents. Similar phenomena were observed for other metal phthalocyanines.

Reduction and oxidation potentials of nonperipheral arylsulfanyl-substituted metal-free phthalocyanines and for those having a central metal of cobalt (Co), nickel (Ni), copper (Cu), zinc (Zn), and lead (Pb) were summarized. The CVs of

Central metal	Potential / V vs. Ag/AgCl							
	Reduction					Oxidation		
Octakis[(4-metylphenyl)tio]phthalocyanine-H₂		-1.31	-1.05				0.31	0.58	
Octakis[(4-metylphenyl)tio]phthalocyanine-Co	-1.68	-1.43*		-0.57	0.21		0.55	0.70*
Octakis[(4-metylphenyl)tio]phthalocyanine-Ni	-1.49	-1.32	-1.16	-0.19		0.29	0.57	0.71*
Octakis[(4-metylphenyl)tio]phthalocyanine-Cu		-1.42	-1.13	-0.49*		0.31	0.61	
Octakis[(4-metylphenyl)tio]phthalocyanine-Zn	-1.62	-1.26		-0.70*	0.12		0.53	
Octakis[(4-metylphenyl)tio]phthalocyanine-Pb		-1.29	-1.03	-0.47*	0.19	0.44		
Octakis[(4-methoxyphenyl)tio]phthalocyanine-H₂		-1.31	-1.04				0.31	0.58	
Octakis[(4-methoxyphenyl)tio]phthalocyanine-Co				-0.60	0.17		0.52	0.82
Octakis[(4-methoxyphenyl)tio]phthalocyanine-Ni	-1.49	-1.31	-1.16	-0.18		0.29	0.57	0.68
Octakis[(4-methoxyphenyl)tio]phthalocyanine-Cu	-1.68	-1.43	-1.13			0.28	0.61	
Octakis[(4-methoxyphenyl)tio]phthalocyanine-Zn	-1.61	-1.29			0.06		0.48	
Octakis[(4-methoxyphenyl)tio]phthalocyanine-Pb	-1.54	-1.29	-1.04	-0.47*	0.19	0.44	0.55*	
Octakis[(4-*tert*-butylphenyl)tio]phthalocyanine-H₂		-1.30	-1.03				0.32	0.58	
Octakis[(4-tert-butylphenyl)tio]phthalocyanine-Co	-1.68*	-1.43*		-0.57	0.21		0.53	0.79
Octakis[(4-tert-butylphenyl)tio]phthalocyanine-Ni	-1.53		-0.60	-0.16		0.33	0.59	0.73
Octakis[(4-tert-butylphenyl)tio]phthalocyanine-Cu		-1.43	-1.13			0.30	0.62	
Octakis[(4-tert-butylphenyl)tio]phthalocyanine-Zn		-1.46	-1.19		0.12		0.53	
Octakis[(4-tert-butylphenyl)tio]phthalocyanine-Pb	-1.57*	-1.26	-1.00	-0.35	0.21	0.47	0.69	0.85*

Potentials of reversible wave are midpoint of anodic and cathodic praks for each couple $E_{1/2}$.

*Irreversible peak.

Table 6.
Reduction and oxidation potentials of nonperipheral arylsulfanyl substituted phthalocyanine in o-dichlorobenzene with tetrabutyl ammonium perchlorate.

these compounds exhibited reduction and oxidation potentials, which were in accordance with their central metal (**Table 6**).

The arylsulfanyl substituents in nonperipheral arylsulfanyl-substituted phthalocyanines influence the π electron density in the phthalocyanine ring. The effect of arylsulfanyl groups gives rise to the change of electron density of phthalocyanine ring in the molecule of nonperipheral arylsulfanyl-substituted phthalocyanines. Nonperipheral arylsulfanyl-substituted phthalocyanines exhibit excellent electron transfer properties.

The reduction and oxidation properties of nonperipheral arylsulfanyl-substituted phthalocyanines result from electron transfer from sulfur atoms in the arylsulfanyl substituents at the peripheral positions of phthalocyanine ring to the central metal atom, except in the case of Co as the central metal. In nonperipheral arylsulfanyl-substituted Co phthalocyanines, the irreversible peaks are attributed to the central metal and the reversible waves represent the reduction/oxidation of phthalocyanine ring, including arylsulfanyl groups. It appears that the electron transfer mechanism of nonperipheral arylsulfanyl-substituted phthalocyanines depend on the kind of central metal atom. In particular, the electron transfer mechanism of nonperipheral arylsulfanyl-substituted Co phthalocyanines and nonperipheral arylsulfanyl-substituted Zn phthalocyanines were attributed to reduction and oxidation of their central metal, while those of nonperipheral arylsulfanyl-substituted metal-free phthalocyanines, nonperipheral arylsulfanyl-substituted Cu phthalocyanines, nonperipheral arylsulfanyl-substituted Ni phthalocyanines, and nonperipheral arylsulfanyl-substituted Pb phthalocyanines resulted from HOMO to LUMO electron transitions [20].

3.3 Subphthalocyanines and nonperipheral arylsulfanyl-substituted subphthalocyanines

The CV of subphthalocyanine showed two cathodic peaks at −0.30 and −0.65 V versus Ag/AgCl, and two anodic peaks at 0.82 and −0.62 V versus Ag/AgCl. Subphthalocyanine has two irreversible oxidation and reduction at 0.82 and −0.30 V versus Ag/AgCl, and one pair of reversible reduction potential at −0.64 V versus Ag/AgCl (**Figure 24**).

The reduction and oxidation potentials of subphthalocyanine and its derivatives are summarized (**Table 7**).

In the case of metal phthalocyanines, their substituents influence the π electron environment in the molecule especially the four phenylene rings. The effect of substituents gives rise to the change of electron density of the four phenylene rings in the molecule. Electron transfer properties depend on the kind of the substituents.

While in the case of subphthalocyanine and its derivatives, reduction and oxidation potentials were of various values. However, one irreversible potential certainly appeared around −0.3 V versus Ag/AgCl, of which peaks are attributed to the reduction of the subphthalocyanine ring. The difference of CV between subphthalocyanine derivatives is attributed to the variation of the substituents depends on the subphthalocyanine ring [33].

The CVs of nonperipheral arylsulfanyl-substituted subphthalocyanines show similar shapes (**Figure 25**).

The shapes of hexakis[(4-*tert*-butylphenyl)thio]subphthalocyanine showed cathodic and anodic peaks. The pair of peaks appeared at around −1.69, −1.15, 0.62, and 0.88 V versus Ag/AgCl. Oxidation and reduction potentials of nonperipheral arylsulfanyl-substituted subphthalocyanines were summarized (**Table 8**).
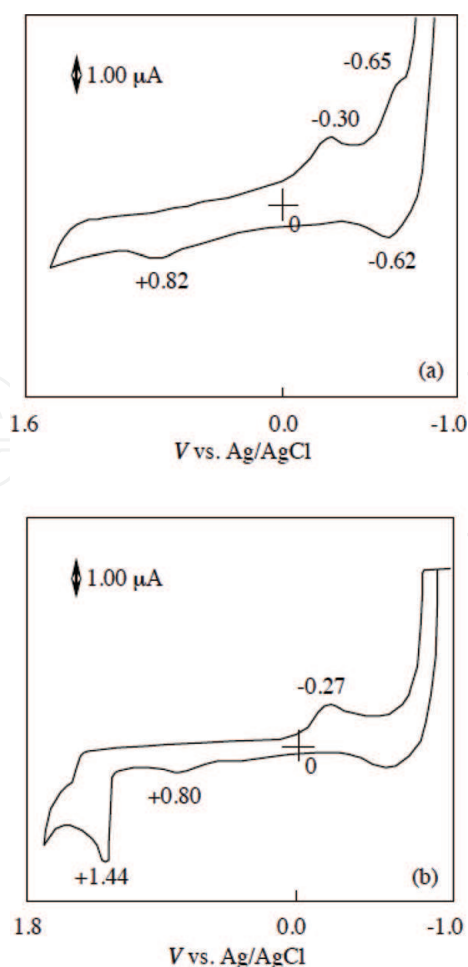
Figure 24.
Cyclic voltammograms of unsubstituted subphthalocyanine and dodecylkis(thiobutyl)subphthalocyanine in acetonitrile with 0.1 mol cm^{-3} tetrabutylammonium perchlorate. (a) unsubstituted SubPC, (b) dodecylkis (thiobutyl)subphthalocyanine.

As mentioned above, in general, metal phthalocyanines having transition metal behave as electrochemically irreversible, and exhibit reduction and oxidation properties resulting from interaction between the phthalocyanine ring and their central metal. The oxidation potential is about 1.0 V versus SHE. The reduction potential occurs between -0.3 and -0.8 V versus SHE. Electrons are added either to the molecular orbital of the phthalocyanine ring or the central metal, depending on the reduction and oxidation potential for reduction process.

As mentioned above, an irreversible reduction appeared around -0.3 V versus Ag/AgCl for subphthalocyanines [33]. The irreversible peaks of subphthalocyanines are attributed to the reduction of the subphthalocyanine ring. The reduction and oxidation potentials of subphthalocyanines result from their substituents.

CVs of nonperipheral arylsulfanyl-substituted subphthalocyanines differ in terms of shape from subphthalocyanine; hexakis[(4-*tert*-butylphenyl)thio] subphthalocyanine has many reduction and oxidation peaks. These phenomena mean that the substituents variedly act in accordance with their electro-donating property for methyl, methoxy, and *tert*-butyl, although they do not demonstrate the effect as chromophores. The substituents of nonperipheral arylsulfanyl-substituted subphthalocyanines are affected more by subphthalo-cyanines than phthalocyanine ring above mentioned corresponding octakis (arylsulfanyl)phthalocyanines [34]. Nonperipheral arylsulfanyl-substituted subphthalocyanines show many reduction potentials. Nonperipheral arylsulfanyl-substituted subphthalocyanines are acceptable electrons in the

Compound	Potential / V vs. Ag/AgCl			
	Reduction		Oxidation	
Hexakis(thiobutyl)hexafuluoro-subphthalocyanine	0.56*	-0.28*	0.83	
DE^b	0.03			
Hexakis(thiophenyl)hexafuluoro-subphthalocyanine	-0.27*		0.80*	1.44*
Dodecylkis(thiobutyl)hexafuluoro-subphthalocyanine	-0.21*	-0.37*	0.18*	
Dodecylkis(thiophenyl)hexafuluoro-subphthalocyanine	-0.57*	-0.46*	0.18*	
Subphthalocyanine	-0.64	-0.03*	0.82*	
ΔE**	0.03			

Potentials of reversible wave are midoopoint potential of anodic and cathodic peaks for each couple $E_{1/2}$.

* Irreversible peak.

** The anodic peak to cathodic peak separation for reversible couple.

Table 7.
Reduction and oxidation potential of subphthalocyanines.
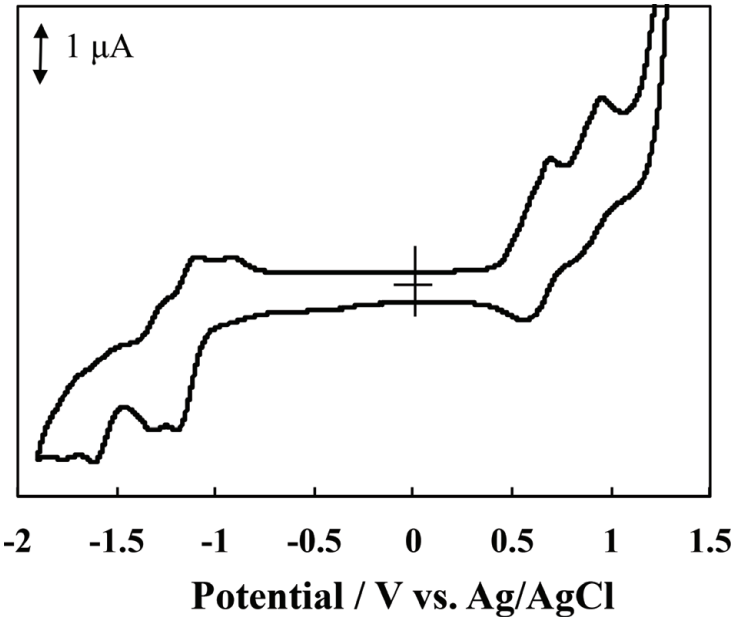
Figure 25.
Cyclic voltammogram of hexakis[(4-tert-butyl)thio]subphthalocyanine in o-dichlorobenzene with $0.1 \ mol \ cm^{-3}$ tetrabutylammonium perchlorate.

Compound	Potential / V vs.Ag/AgCl in dichloromethane Solvent						
	Reduction					Oxidation	
Hexakis[(4-metylphenyl)thio]subphthalocyanine	-1.74	-1.56	-1.28	-1.14	-0.92*	0.62	0.90
Hexakis[(4-*tert*-butylphenyl)thio]subphthalocyanin		-1.69	-1.15	-0.90*		0.62	0.88
Hexakis[(4-metylphenyl)thio]phthalocyanine		-1.25	-0.86	-0.46		0.38	
Subphthalocyanine			-1.31			0.75	
	Potential / V vs.Ag/AgCl in chloroform Solvent						
	Reduction		Oxidation				
Hexakis[(4-metylphenyl)thio]subphthalocyanine	-1.81	-1.43*	0.80*				
Hexakis[(4-tert-butylphenyl)thio]subphthalocyanine	-1.81		0.74*				
Subphthalocyanine	-1.52*	-1.20*	0.81*				

Potentials of reversible wave are midpoint of anodic and cathodic praks for each couple $E_{1/2}$.

*Irreversible peak.

Table 8.
Reduction and oxidation potential of nonperipheral arylsulfanyl-subphthalocyanine and asymmetric 3:1 phthalocyanine, hexakis(arylsulfanyl)phthalocyanine in o-dichlorobenzene or chloroform with $0.1 \ mol \ cm^{-3}$ tetrabutylammonium perchlorate.

subphthalocyanine ring compare with corresponding octakis(arylsulfanyl) phthalocyanines [34].

CV of asymmetric 3:1 type phthalocyanine, hexakis[(4-methylphenyl)thio] phthalocyanine shows peaks at −1.25, −0.86, 00.46, and 0.38 V versus Ag/AgCl. These data are similar to octakis[(4-methylphenyl)thio]phthalocyanine.

4. Conclusion

Electrochemical measurements were performed cobalt phthalocyanine-4,4′,4″ 4‴-tetrasulfonic acids, cobalt phthalocyanine-2,3,9,10,16,17,23,24-octacarboxylic acids, cobalt 2,3,9,10,16,17,23,24-octakis(hexoxymethyl)phthalocyanine, and cobalt anthraquinocyanine in order to examine their electron transfer abilities and electrochemical mechanism.

The CVs of zinc bis(1,4-didecylbenzo)-bis(3,4-pyrido)porphyrazine and its regioisomers showed different oxidation and reduction potentials. After quaternation, the shapes of CVs appeared clearly. It is though that electron transfer ability has been increased remarkably by acquisition of cation groups.

The electron transfer properties of nonperipheral arylsulfanyl-substituted phthalocyanines were shown to be excellent estimated. The effect of arylsulfanyl groups gives rise to be significant.

Electron transition in nonperipheral arylsulfanyl-substituted Co phthalocyanines and nonperipheral arylsulfanyl-substituted Zn phthalocyanines are attributed to reduction and oxidation of their central metal, whereas, in nonperipheral arylsulfanyl-substituted metal-free phthalocyanines, nonperipheral arylsulfanyl-substituted Cu phthalocyanines, nonperipheral arylsulfanyl-substituted Ni phthalocyanines and nonperipheral arylsulfanyl-substituted Pb phthalocyanines, electron transfer results from HOMO to LUMO electron transition.

For subphthalocyanine and its derivatives, reduction and oxidation potentials were various values. The difference of CV between subphthalocyanine derivatives is attributed to the variation of the substituents depends on the subphthalocyanine ring.

Nonperipheral arylsulfanyl-substituted subphthalocyanines show many reduction potentials. Nonperipheral arylsulfanyl-substituted subphthalocyanines are acceptable electrons in the subphthalocyanine ring, meaning that the nonperipheral arylsulfanyl-substituted subphthalocyanines have good electron transfer properties.

Asymmetric 3:1 type phthalocyanine, hexakis[(4-methoxyphenyl)thio]phthalocyanine has similar properties of previous reported phthalocyanines.

These results suggest that phthalocyanines will be appropriate materials for use in the next generation photosensitize for PDT and DSSCs.

Acknowledgements

Author details

Keiichi Sakamoto[1,2]

1 Department of Sustainable Engineering, College of Industrial Technology,
Nihon University, Chiba-ken, Japan

2 Academic Major of Applied Molecular Chemistry, Graduate School of Industrial
Technology, Nihon University, Chiba-ken, Japan

*Address all correspondence to: sakamoto.keiichi@nihon-u.ac.jp

IntechOpen

References

[1] Hirohashi R, Sakamoto K, Ohno-Okumura E, editors. Phthalocyanines as Functional Dyes. Tokyo: IPC; 2004. pp. 1-22

[2] McKeown NB. Phthalocyanine Materials, Synthesis, Structure and Function. Cambridge: Cambridge University Press; 1998. pp. 1-11

[3] Lezonoff CC, Lever ABP, editors. Phthalocyanines. Vol. 1. Ontario: VCH Publishers; 1989. pp. 5-6

[4] Moser FH, Thomas AL. The Phthalocyanines. Vol. 1. Florida: CRC Press; 1983. pp. 1-3

[5] Moser FH, Thomas AL. Phthalocyanine Compounds. New York: Chapman & Hall; 1963. pp. 1-9

[6] Likyanets EA, Nemykin VN. Journal of Porphyrins and Phthalocyanines. 2010;**14**:1-40

[7] Campidell S, Ballesteros B, Filoramo A, Diaz D, de la Torre G, Torres T, et al. Journal of the American Chemical Society. 2008;**139**:11503-11509

[8] de la Torre G, Vazques P, Torres T. Chemical Reviews. 2004;**104**:3723-3750

[9] Cid JJ, Jang SR, Nazeeruddin MK, Matinez-Ferrero E, Ko J, Graetzel M, et al. Angewandte Chemie, International Edition. 2007;**46**:8358-8362

[10] Sakamoto K, Ohno-Okumura E. Materials. 2009;**2**:1127-1180

[11] Pinzon JR, Plnska-Brzezinska ME, Cadona CM, Athans AJ, Gayathri SS, Guldi DM, et al. Angewandte Chemie, International Edition. 2008;**47**:4173-4176

[12] Drumus M, Taman H, Gol C, Ahsen V, Nykong T. Dyes and Pigments. 2011;**91**:153-156

[13] Ichikawa M, Kobayashi K, Koyama T, Taniguchi Y. Thin Solid Films. 2007;**515**:3932-3935

[14] Shao J, Thomas A, Han B, Hansen CA. Journal of Porphyrins and Phthalocyanines. 2010;**14**:133-141

[15] Sharma U, Verma PK, Kumar V, Bala M, Singh B. Chemistry–A European Journal. 2011;**17**:5903-5907

[16] Bertagnolli H, Krishnan V, Youssef TE, Hanack M. Journal of Porphyrins and Phthalocyanines. 2011;**15**:598-601

[17] Sakamoto K, Kato T, Cook MJ. Journal of Porphyrins and Phthalocyanines. 2001;**5**:742-750

[18] Sakamoto K, Kato T, Kawaguchi T, Ohno-Okumura E, Urano T, Yamaoka T, et al. Journal of Photochemistry and Photobiology A: Chemistry. 2002;**153**:245-253

[19] Sakamoto K, Ohno-Okumura E, Kato T, Soga H. Journal of Porphyrins and Phthalocyanines. 2010;**14**:47-54

[20] Sakamoto K, Furuya N, Soga H, Yoshino S. Dyes and Pigments. 2013;**96**:430-434

[21] Sakamoto K, Yoshino S, Takemoto M, Furuya N. Journal of Porphyrins and Phthalocyanines. 2013;**17**:605-627

[22] Haywood-Small SL, Vernon DI, Griffiths J, Schofield J, Brown SB. Biochemical and Biophysical Research Communications. 2006;**339**:569-576

[23] Komiarov AN, Makarov DA, Yuzhakova OA, Savvina LP, Kuzznetsiva NA, Kaliya OL, et al. Macroheterocycles. 2012;**5**:169-174

[24] Jori G. Photochemistry and Photobiology. 1990;**52**:439-443

[25] Idown M, Loewenstein T, Hastall A, Nykong T, Schlettwein d. Journal of Porphyrins and Phthalocyanines. 2010; **14**:142-149

[26] Sakamoto K, Ohno E. Journal of the Society of Dyers and Colourists. 1996; **112**:368-374

[27] Ohno E, Sakamoto K. The Chemical Society of Japan. 1995;**1995**:730-735

[28] Sakamoto K, Ohno-Okumura E, Kato T, Watanabe M, Cook MJ. Dyes and Pigments. 2008;**78**:213-218

[29] Sakamoto K, Kato T, Ohno-Okumura E, Watanabe M, Cook MJ. Dyes and Pigments. 2005;**64**:63-71. DOI: 10.1016/j.dypig.2007.12.004

[30] Sakamoto K, Watabiki S, Yoshino S, Komoriya T. Journal of Porphyrins and Phthalocyanines. 2017;**21**:658-664

[31] Sakamoto K, Yoshino S, Takemoto M, Sugaya K, Kubo H, Komoriya T, et al. American Journal of Analytical Chemistry. 2014;**5**:1037-1045

[32] Claessens CG, Gonzalez-Rodriguez D, Torre T. Chemical Reviews. 2002; **102**:835-853

[33] Ohno-Okumura E, Sakamoto K, Kato T, Hatano T, Fukui K, Karatsu T, et al. Dyes and Pigments. 2002;**53**:57-65

[34] Sakamoto K, Yoshino S, Takemoto M, Sugaya K, Kubo H, Komoriya T, et al. Journal of Porphyrins and Phthalocyanines. 2015;**19**:688-694